MOLECULAR COMMUNICATIONS IN VESSEL-LIKE DIFFUSIVE CHANNELS

by

Meriç Turan

B.S., Computer Engineering, Istanbul Technical University, 2017

Submitted to the Institute for Graduate Studies in
Science and Engineering in partial fulfillment of
the requirements for the degree of
Master of Science

Graduate Program in Computer Engineering

Boğaziçi University

2019

ACKNOWLEDGEMENTS

First of all, I would like to thank my thesis supervisor Prof. Tuna Tuğcu for his patience, for the opportunities he provided to me, and for his contribution to this thesis. I would also like to thank Assoc. Prof. Ali Emre Pusane for his valuable comments and ideas.

I also send my deepest gratitude to Dr. H. Birkan Yılmaz and Dr. Mehmet Şükrü Kuran for their supports. I would not be able to prepare this thesis without their help for sure. I also thank all of the members of the Nanonetworking Research Group (NRG).

I also sincerely thank Assoc. Prof. Chan-Byoung Chae and his team in Yonsei University for their hospitality.

I am also very thankful to my best friend, M.D. Ender İğneci, for both his moral support and contribution in the medical sense to this thesis.

I am also very grateful to my girlfriend, Elif İnan, for her love and smiling face.

Last but definitely not the least, I am very grateful to my parents Özgül Turan and Metin Turan, and my sister Zeynep Turan for their unlimited support, encouragement, and patience during not only my master study, but also my whole life.

This thesis was partially supported by the Scientific and Technological Research Council of Turkey (TUBITAK) under Grant number 116E916.

ABSTRACT

MOLECULAR COMMUNICATIONS IN VESSEL-LIKE DIFFUSIVE CHANNELS

Molecular communication via diffusion is based on relaying information over a diffusive channel. The design of this diffusive channel is a vital issue. In this thesis, diffusion in the vessel-like environment, which is composed of a cylindrical environment resembling a blood vessel encompassing all the components of the communication system, is studied. Even though the range of communication increases in such environments due to the effect of the blood flow, vessel-like environments are not very suitable for analytical analysis. Therefore, many works, which considered vessel-like environment as the communication environment, are based on the simulation results rather than the analytical results. In order to fill this gap in the literature and to be able to localize the transmitter, we derive the analytical formulation of the channel model for diffusion-dominated movement, considering ring-shaped observing receivers and Poiseuille flow. Then, we derive formulations using this channel model for two different application scenarios, known and unknown emission time. A single receiver is used to localize the transmitter for known emission time, whereas two receivers are used for unknown emission time. Besides, as an alternative to signal-to-noise ratio (SNR), we propose MOL-Eye diagram and some metrics of this diagram (e.g., counting SNR) for the performance evaluation of a molecular signal. Also, binary concentration shift keying with consecutive power adjustment (BCSK-CPA) modulation technique is proposed to decrease destructive inter-symbol interference (ISI) effect and increase constructive ISI effect. Moreover, within the vessel-like environments, different values for the components of the environment (e.g., receiver, flow) are investigated. Lastly, partially covering receiver is proposed as a new type of receiver, and channel model of such environment is devised. Finally, all of the devised frameworks are validated with custom-made simulators.

ÖZET

DİFÜZYON BAZLI DAMARSI ORTAMLARDA MOLEKÜLER HABERLEŞME

Difüzyon ile moleküler haberleşme difüzyon bazlı bir kanal üzerinde bilgi iletimine dayanmaktadır. Bu kanalın tasarımı kritik bir konudur. Bu tezde, haberleşme sisteminin bütün parçalarını içerisinde bulunduran ve kan damarına benzeyen silindirik bir ortam olan damarsı ortam çalışılmıştır. Haberleşme mesafesinin kan akışı sebebiyle bu tarz ortamlarda artıp uzun mesafeli uygulamalara olanak tanımasına rağmen, analitik analizler için çok uygun bir ortam değillerdir. Bu sebeple, haberleşme ortamı olarak damarsı ortamı kullanan çalışmaların bir çoğu analitik sonuçlardansa simülasyon sonuçlarına dayanmaktadır. Bu boşluğu doldurmak ve göndericinin yerini tespit etmek maksadıyla, yüzük şeklinde pasif alıcı ve Poiseuille akışını dikkate alarak, difüzyon bazlı hareketin hakim olduğu kanal modelinin analitik formülünü çıkardık. Sonrasında, bu kanal modelini kullanarak bilinen ve bilinmeyen salınım başlama zamanı olmak üzere iki farklı uygulama senaryosu için formül çıkardık. Bilinen salınım zamanı için göndericinin yerini tek bir alıcı kullanarak tespit edebilirken, bilinmeyen salınım zamanı için iki alıcı kullanarak göndericinin yerini tespit ettik. Bunlar dışında, sinyal gürültü oranı metriğine alternatif olarak, *MOL-Eye* diyagramı ve bu diyagramın bazı metriklerini (biriken sinyal gürültü oranı gibi) moleküler sinyalin performansının hesaplanması maksadıyla önerdik. Ayrıca, *binary concentration shift keying with consecutive power adjustment* (BCSK-CPA) adını verdiğimiz modülasyon tekniğini yıkıcı girişimin etkisi azaltıp, yapıcı girişimin etkisini arttırması amacıyla önerdik. Bunlar dışında, damarsı ortamda farklı alıcı ve akış gibi bileşenler kullanıldı. Son olarak, kısmı kapsayan alıcı yeni bir alıcı tipi olarak önerilmiş ve bu ortamın kanal modeli tasarlanmıştır. En sonunda, oluşturulan yapıların tamamı özel yapılmış simülatör ile doğrulanmıştır.

TABLE OF CONTENTS

LIST OF FIGURES

LIST OF TABLES

LIST OF SYMBOLS

$\mathrm{A}(\cdot)$	Area of the receiver
$\boldsymbol{C}_k$	Vector representing the consecutive bit-1 values within the previous m symbols at the kth symbol slot (used in BCSK-CPA)
d_1	Distance between the transmitter and the closest receiver
d_2	Distance between the transmitter and the second receiver
d	Distance from the emission point
D	Diffusion coefficient
D_e	Effective diffusion coefficient
$d_{R,i}$	Distance between the transmitter and the closest part of the receiver
$d_{R,i} + w$	Distance between the transmitter and the most far part of the receiver
$\mathbf{E}(\cdot)$	Expectation operator
$F_{\mathrm{hit}}(t)$	Hitting rate of the molecules at time t
$\boldsymbol{H}_k^m$	Vector representing the symbol values of the previous m symbols at the kth symbol slot (used in BCSK-PA)
$\mathtt{HR}(r_a\|t)$	The ratio of the hitting molecules whose axial distances are less than an arbitrary radius r_a to all hitting molecules within time t
m	ISI window length
n_0	Number of released molecules for bit-0 transmission
n_1	Number of released molecules for bit-1 transmission
$n_1^{\boldsymbol{C}_k}$	Number of molecules to emit when the number of consecutive bit-1s is equal to $\boldsymbol{C}_k$
$N_{\mathrm{residual}}[k]$	Expected number of residual molecules at kth symbol duration
$N^{\mathrm{Rx}}[k]$	Number of received molecules at kth symbol duration
$N^{\mathrm{Rx}}(r\|t)$	Total number of hitting molecules whose axial distances are less than r within time t
$N^{\mathrm{Tx}}[k]$	Number of transmitted molecules at kth symbol duration

$p(d,t)$	Probability for a molecule to be at a certain d distance from the emission point at time t
$\mathbf{P}_{\mathrm{d}}(\Omega_i,t)$	Probability for a molecule to be sensed by Ω_i at time t
$\mathbf{P}_e$	Probability of error
Pe	Péclet number
p_i	Mean fraction of emitted molecules that are received during the ith following symbol slot
r_c	Distance between messenger molecule and the central axis of the vessel
r_v	Radius of the vessel
$S[k]$	Transmitted symbol at kth symbol duration
$\hat{S}[k]$	Received symbol at kth symbol duration
v_m	Average flow velocity
$v_{\max}$	Maximum flow velocity
$v_{\min}$	Minimum flow velocity
v_{pf}	Poiseuille flow velocity
v_{uf}	Uniform flow velocity
t_p	Peak time
$t_{p,1}$	Analytical peak time that first receiver observes
$t_{p,1}^{n_1}$	Measured peak time by the first receiver
$t_{p,2}$	Analytical peak time that second receiver observes
t_s	Symbol duration
w	Width of the receiver
x_f	Location of the molecule after reflection occurred in the x axis
y_f	Location of the molecule after reflection occurred in the y axis
z_f	Location of the molecule after reflection occurred in the z axis
σ^2	Variance
$\Delta\overrightarrow{r}$	Total displacement of the molecules
Δt	Simulation step time
ΔX	Displacement in the x axis
$\Delta X_{\mathrm{diffusion}}$	Displacement in the x axis caused by diffusion

ΔX_{Pflow}	Displacement in the x axis caused by Poiseuille flow effect
ΔX_{Uflow}	Displacement in the x axis caused by uniform flow effect
$\Delta Y_{\text{diffusion}}$	Displacement in the y axis
$\Delta Z_{\text{diffusion}}$	Displacement in the z axis
λ	Threshold value
μ	Mean
$\mathscr{N}(\cdot, \cdot)$	Gaussian distribution
$\Phi(\cdot)$	Ratio of partially covering receiver to the cross sectional area of the vessel
Ω_i	ith receiver
$\triangle d_{2,1}$	Distance difference between the transmitter and the receivers
$\triangle t_{2,1}$	Mean peak time difference that second and first receivers observe

LIST OF ACRONYMS/ABBREVIATIONS

1D	One dimensional
2D	Two dimensional
3D	Three dimensional
AbM	Amplitude-based modulation
BER	Bit-error-rate
BCSK	Binary concentration shift keying
BCSK-CPA	Binary concentration shift keying with consecutive power adjustment
BCSK-PA	Binary concentration shift keying with power adjustment
BMFSK	Binary molecular frequency shift keying
BMoSK	Binary molecular shift keying
CSK	Concentration shift keying
CSNR	Counting signal-to-noise ratio
FbM	Frequency-based modulation
ISI	Inter-symbol interference
K-S	Kolmogorov-Smirnov
MaxEH	Maximum eye height
MC	Molecular communication
MCvD	Molecular communication via diffusion
MFSK	Molecular frequency shift keying
MLE	Maximum likelihood estimation
MM	Messenger molecule
MoSK	Molecular shift keying
MTbM	Molecule type-based modulation
QCSK	Quadrature concentration shift keying
QMFSK	Quadrature molecular frequency shift keying
QMoSK	Quadrature molecular shift keying
RF	Radio frequency
SER	Symbol-error-rate

SINR	Signal-to-noise-interference ratio
SNR	Signal-to-noise ratio
TbM	Timing-based modulation

1. INTRODUCTION

Nanonetworking is a communication paradigm that focuses on communication between nano-scale devices, whose sizes are comparable to biological cells. Due to their small sizes, medical applications in *in vivo* environments are expected to be one of the most prominent and driving application domains for these devices. However, an *in vivo* environment is quite different from the classical radio frequency (RF) communication environment, and development of novel communication systems for this environment are needed. One such system is the molecular communication via diffusion (MCvD) that is based on relaying information over a diffusion channel using special molecules, called messenger molecules (MM) [1].

MCvD is one of the prominent communication systems in the greater context of nanonetworking, which aims to enable communication between cell-sized machines in *in vivo* applications. In MCvD, information is carried via a signal of MMs between the transmitter and the receiver cells, all of which reside inside a fluid environment [1]. Until recently, most of the work focusing on MCvD systems have assumed an unbounded free diffusion environment that consists of only the communicating pair (i.e., transmitter and receiver) and the MMs used for communication. Although such environments are extremely suitable for analytical analysis of the various aspects of this unique communication system, their applicability is somewhat limited for biomedical applications.

A more realistic alternative to the unbounded free diffusion environment is the vessel-like environment [2,3], which is composed of a cylindrical environment resembling a blood vessel, encompassing all components of the system. Additionally, there is a flow element, which affects the movement of the MMs. These differences change the channel model of the MCvD system considerably. In the literature, several communication topology are proposed for such environments, based on the type of the receiver and the nature of the flow. The receivers are generally absorbing [4–6] or observing [7], with respect to the MMs passing through, while being either fully [3, 4, 6] or partially [5, 8]

covering the cross section of the cylindrical environment. Moreover, the flow can be either non-existent [9], steady uniform [10], or Poiseuille flow [11].

The main contribution of this thesis can be divided into three main categories as follows:

(i) Analytical formulations for the transmitter cell localization are derived for the vessel-like environment.
(ii) MOL-Eye diagram is proposed for the performance evaluation of a molecular signal.
(iii) Binary concentration shift keying with consecutive power adjustment (BCSK-CPA) modulation technique is proposed to decrease the destructive inter-symbol interference (ISI) effect and increase the constructive ISI effect.
(iv) Partially covering receiver is introduced and distribution of the hitting location of MMs is analyzed with the aim of channel modeling.

1.1. Localization of The Transmitter Cell

In the molecular communication literature, some former works have focused on distance estimation between the transmitter and the receiver cells. To the best of our knowledge, distance estimation inside a vessel-like environment with Poiseuille flow has not been examined in the literature. Poiseuille flow is a type of parabolic flow that represents the pressure-induced flow of an incompressible viscous fluid in a long narrow duct. For the localization of the transmitter, we first study the channel model of a vessel-like environment with Poiseuille flow in the MCvD system for diffusion dominated movement. Then, we develop an analytical model to localize the transmitter for two different application scenarios. In the first application scenario, we assume that receiver knows the emission time, and consequently it can precisely measure the peak time. In the second application scenario, we assume that the receiver does not know the emission time, so it cannot measure the peak time.

We focus on the transmitter localization problem, since it is critical for several MCvD applications, such as detection of abnormal or unhealthy cells in the vicinity of the blood vessels. We consider multiple ring-shaped receivers (i.e., patch receivers) with observing characteristics and a flow component that resembles the blood vessel environment. In the literature, various flow models are used for such environments considering different types of blood vessels. In this thesis, we focus on Poiseuille flow, which defines the flow profile in blood vessels [12, 13].

1.2. Performance Evaluation of a Molecular Signal

The performance of an MCvD system is mostly evaluated using the signal-to-noise ratio (SNR), bit-error-rate (BER), or channel capacity. Less considerably, other metrics such as symbol-error-rate (SER), signal-to-interference ratio (SINR), channel impulse response, and channel capacity considering transmitter energy budget have also been used. Among the three main metrics mentioned above (i.e., SNR, BER, and channel capacity), BER and channel capacity are defined in the context of MCvD. To the best of our knowledge, the physical meaning of SNR and its calculation is not elaborated in detail in this new domain. In RF communication, as an alternative to SNR and SINR, a plot called eye diagram is also used to evaluate the performance of a signal. Different features of this diagram are used to measure various signal characteristics. For example, eye opening is used for noise analysis, eye width is used for jitter analysis, and eye closure is used for ISI analysis.

Inspired by the eye diagram, we propose a new diagram that we call MOL-Eye diagram to evaluate the performance of a molecular signal in this thesis. In more detail, we propose three new metrics to evaluate the performance of an MCvD system based on the MOL-Eye diagram, and named them as maximum eye height (MaxEH), standard deviation of the number of received molecules, and counting SNR (CSNR). Then, the validity of these metrics are evaluated by comparing two different modulation techniques. The first modulation technique is binary concentration shift keying (BCSK) [14, 15], whereas the other one is BCSK with consecutive power adjustment (BCSK-CPA). BCSK-CPA is proposed in this thesis and inspired by BCSK with power

adjustment (BCSK-PA) modulation technique [16,17]. According to the simulation results, the three proposed metrics successfully indicate that BCSK-CPA outperforms BCSK modulation technique. Finally note that, even though we consider a vessel-like environment as the communication environment, the MOL-Eye diagram and the proposed performance metrics can also be applied to free diffusion environments.

1.3. Partially Covering Receiver

Most of the research conducted regarding MCvD in vessel-like environment assumes that a hypothetical receiver covers the vessel in its whole cross sectional area, which we name as fully covering receiver. Since such a hypothetical receiver also blocks the flow, we propose another type of receiver that only covers some portion of the vessel's cross sectional area, and we name it as partially covering receiver. To this end, we analyze the distribution of hitting location of MMs within the context of MCvD with the aim of channel modeling. The distribution of these molecules is analyzed in two parts, namely, angular distribution and radial distribution. For the angular distribution analysis, firstly, the receiver is divided into 180 slices. Then, the mean of hitting molecules, the standard deviation of hitting molecules, and the coefficient of variation values of these slices are analyzed. For the radial distribution analysis, Kolmogorov-Smirnov (K-S) test is applied for two different significance levels (i.e., %5 and %1 significance levels). Also, two different implementation strategies of the reflection from the vessel surface (i.e., rollback and elastic reflection) are compared and the mathematical representation of elastic reflection is given.

1.4. Literature Survey

In the literature, several molecular communication (MC) systems are proposed, such as communication via diffusion [1, 15, 18–21], microtubules [22–25], and calcium signaling [20, 26, 27]. In intracellular MC using microtubules, molecular motor proteins are used to transport the information particles from the transmitter to the receiver. In more detail, molecular motors, namely, kinesins and dyneins, transport molecules along cytoskeletal tracks within eukaryotic cells. Also, the effective range of this com-

munication system is regarded as short. In calcium signaling, communication occurs through gap junctions, which are channels between cells. Cells communicate through gap junctions by sharing calcium ions and IP3 molecules. Also, the effective range of the communication is regarded as medium in calcium signaling. In MCvD, certain molecules are transmitted from the transmitter to the receiver and propagation of these molecules is assured by diffusion, and the effective range of the communication is also regarded as medium. In this thesis, MCvD is considered as MC system due to the enormous number of potential applications.

Many different diffusion environments are considered in MCvD. These environments can be divided into two main categories, namely, unbounded and bounded environment. In an unbounded environment, there are only communicating devices (i.e., transmitters and receivers) and the molecules to relay the information. Even though unbounded environments are very convenient to analyze the communication environment analytically [21, 28, 29], it is unpractical for biomedical applications such as targeted drug delivery [30]. In that sense, we consider a bounded vessel-like environment, which is basically a cylindrical environment and closely resembles the inside of a blood vessel [3, 4, 31–33]. Unlike the unbounded diffusion environment, the molecules are bounded by the walls of the vessel, and upon impact with these walls, they are either reflected or absorbed, depending on the environmental model in the vessel-like environment. Since these walls constrain the movement of the molecules, the effective range of the communication system greatly increases. In other words, more molecules hit the receiver.

Also, within the vessel-like environments, the components of the communication environment may vary from one communication topology to another. Before designing the vessel-like environments, it is important to consider the type of the receiver and flow as well as other parameters such as radius of the vessel, type of the messenger molecule, and diffusion coefficient. While designing the communication environment in vessel-like channel, one of the most important aspect is the type of the receiver [34]. Receivers can be categorized by their shape and their characteristics. Their shape can be circular [4, 6, 7], spherical [3, 35], and square-like [8]. They can also fully [3, 4, 6]

or partially [5, 8] cover the cross section of the vessel. Moreover, the receivers can be absorbing [4–6], observing [7], or temporarily binding [36] with respect to the molecules passing through them. In this thesis, excluding the temporarily binding receiver, all of the mentioned receiver types are considered.

Another important aspect while designing a communication environment in vessel-like channel is the type of the flow. There are three types of fluid flows in pipes, namely, laminar, turbulent, and transitional flow [37]. In the laminar flow, there is no mixing between the layers of the pipe (i.e., layers of the flow are parallel to each other). In the turbulent flow, the fluid moves in an unstable manner between the layers of the pipe. Lastly, the transitional flow is the mixture of laminar and turbulent flow. In blood vessels, the blood moves according to the hemodynamics. Even though the blood is a complex liquid (i.e., non-Newtonian fluid), laminar flow is the normal condition for blood flow throughout most of the circulatory system, so there is a tendency to have laminar flow in vessels [12]. Therefore, laminar flow is considered as the type of the flow in vessel-like environments in this thesis. Moreover, laminar flow also has different types, namely, uniform flow, Poiseuille flow, and Couette flow. The velocity of the flow is the same in all layers of the vessel in uniform flow. In Poiseuille flow, the flow in the center (in terms of radius) of the vessel is high. This high rate of flow decreases in stages towards the sides of the vessel and becomes zero at the border of the vessel. Couette flow is the reverse of the Poiseuille flow. In other words, the flow rate is higher at the sides, and zero at the center. Since it is shown that the blood does not move according to the Couette flow [12], we ignore it in this thesis. Considering the proposed flow types, we investigate two of them, uniform flow [4, 10] and Poiseuille flow [7, 11] as well as no flow effect [5, 9].

One of the advantages of vessel-like environment compared to the unbounded environment is its suitability to model significant *in vivo* applications. One such application is localizing the abnormal and unhealthy cells, which is an extremely challenging and vital topic to cover. There are some former works in the literature that have focused on distance estimation between the transmitter and the receiver. In [38], diffusion environment is considered as one dimensional (1D), and the effect of the flow is not consid-

ered. Also, peak concentration is used as the estimation method, and synchronization between the transmitter and the receiver is not needed. Even though their work does not need synchronization between the communicating pairs, the authors considered a very simple communication environment. In [39], unbounded diffusion environment is considered, but the effect of the flow is ignored. As the estimation method, they proposed using peak time and energy. However, the authors assume that the receiver knows the peak time, so their work requires perfect synchronization between the transmitter and the receiver. In [40], Noel *et al.* assume unbounded three dimensional (3D) communication environment, uniform flow, and passive receiver. Several channel parameters, including the distance, have been estimated using a maximum likelihood estimation (MLE) method. In [41], channel parameter estimation in an inverse Gaussian distributed channel with positive flow in a 1D diffusive channel is studied. For the estimation, the authors use MLE method. Also, the authors assume that receiver is aware of the release time of the molecules because it is encoded inside the messenger molecules. In [42], Mosayebi *et al.* assume two dimensional (2D) bounded environment with uniform flow. As seen, none of these works have assumed a bounded 3D environment with laminar flow.

Also, there are several proposed modulation techniques in the MCvD literature [43]. These techniques can be categorized under five types. First and most commonly investigated one is the amplitude-based modulations (AbM). In AbM, the concentration of the received molecules is used to represent the data. The most common AbM technique is concentration shift keying (CSK) [15]. CSK also has its variations such as binary CSK (BCSK) and quadrature CSK (QCSK), based on the number of the amplitude levels. Second important approach is molecule type-based modulations (MTbM). In MTbM, the type of the molecule represents the intended data. The most common MTbM technique is molecular shift keying (MoSK) [15]. MoSK also has its variations such as binary MoSK (BMoSK) for binary channel and quadrature MoSK (QMoSK) for quadruple channel. Third approach is frequency-based modulations (FbM). In FbM, data is represented by benefiting from the frequency changes of the carrier wave. The most common FbM technique is called molecular frequency shift keying (MFSK). MFSK for two distinct frequencies are called as binary MFSK

(BMFSK), whereas MFSK for four distinct frequencies are called as quadrature MFSK (QMFSK). Another type of modulation technique is timing-based modulations (TbM). In TbM, information is modulated based on the timing of the molecule emissions [44]. The last type of modulation technique is realization with isomers. Realization with isomers is less feasible, especially for *in vivo* environments, compared to the other modulation technique types because the used molecules are extremely flammable. In this thesis, we consider AbM, specifically BCSK due to its lower complexity.

There are also several metrics in the literature for evaluating the performance of a molecular signal. The performance of an MCvD system is generally evaluated using SNR, BER, or channel capacity. Less prominently, other metrics such as SER, SINR, channel impulse response, and channel capacity considering transmitter energy budget have also been used. Previous studies, which consider symbols that are representing multiple bits of information, utilize SER instead of BER [14,45]. Other works that take into account the effect of interfering sources (e.g., ISI, co-channel interference, adjacent channel interference) over the system use SINR instead of SNR [46,47]. In [48–50], the authors use channel impulse response to show the effectiveness of the proposed signal shaping method. Lastly, channel capacity can also be expanded to include the energy limitation of the transmitter [21]. Among the presented metrics, only BER and channel capacity are defined in the context of molecular communication, and physical definition of SNR and calculation of SNR are missing for the molecular communication domain. In that sense, by inspiring the eye diagram in RF communication, MOL-Eye diagram is proposed as an alternative metric to the SNR and SINR.

1.5. Contributions of This Thesis

In this thesis, several different communication topology are proposed by changing the type of receivers, namely, absorbing, observing, fully covering, partially covering, and ring-shaped (i.e., patch) receivers, and the type of the flow, namely, non-existent, uniform, and Poiseuille flow. The main contributions of this thesis can be grouped as follows:

(i) Localizing the transmitter in vessel-like diffusive channels.

- Ring-shaped receiver, which can sense either its whole projection area or up to a certain depth inside the vessel, is proposed as a new receiver type.
- A channel model of the MCvD system in a vessel-like environment considering a point transmitter, ring-shaped observing receivers, and Poiseuille flow is developed.
- Analytical formulations for the location estimation of the transmitter are derived by using a single patch receiver when the emission time is known by the receiver.
- Analytical formulations for the peak time and the transmitter location estimation are derived by using two patch receivers when the emission time is not known by the receivers.

(ii) Proposing new metrics for the performance evaluation of a molecular signal.

- Inspired by the eye diagram in classical RF based communications, the MOL-Eye diagram is proposed.
- Utilizing various features of the MOL-Eye diagram, three new metrics for the performance evaluation of a molecular signal, namely, the maximum eye height, standard deviation of received molecules, and CSNR are introduced.
- Based on BCSK, a new power adjustment technique, BCSK-CPA, is proposed to increase the constructive inter-symbol interference (ISI) effect and decrease the destructive ISI effect by decreasing the memory requirement needed in BCSK-PA.

(iii) Introducing partially covering receiver and modeling the vessel-like diffusive channel considering a partially covering receiver.

- Partially covering receiver, which covers some portion of the vessel's cross sectional area, is introduced.
- Two different reflection strategies (i.e., elastic reflection and rollback) are investigated. Mathematical representation of elastic reflection is presented.
- The distribution of messenger molecules over the receiver is analyzed. Distribution analysis is divided into two parts, namely, angular distribution analysis and radial distribution analysis.

- For the cases where uniformity is assured, a channel model is proposed for the partially covering receiver.

1.6. Thesis Outline

This thesis is structured as follows. In Chapter 2, we introduce ring-shaped receiver and localize the transmitter cell in vessel-like diffusive channels. We propose a power adjustment technique, BCSK-CPA, and new performance evaluation metrics for molecular communication in Chapter 3. As the last contribution of this thesis, we introduce partially covering receiver and model the channel considering this new type of receiver in Chapter 4. Finally, we draw the conclusion of this thesis in Chapter 5.

2. TRANSMITTER LOCALIZATION IN VESSEL-LIKE DIFFUSIVE CHANNELS USING RING-SHAPED MOLECULAR RECEIVERS

As a first contribution of this thesis, we derive the analytical formulation of the channel model for diffusion dominated movement, considering ring-shaped observing receivers and Poiseuille flow with the goal of the transmitting cell localization. Then, we derive formulations using this channel model for two different application scenarios. We assume that the emission time is known by the receiver in the first scenario, whereas it is unknown to the receiver in the second scenario. For the first scenario, we successfully localize the transmitter cell using a single receiver. For the second scenario, two receivers are used to localize the transmitter cell. After all, simulations are used to validate the devised analytical framework.

2.1. System Model

In this section, we focus on a vessel-like environment that includes a single point transmitter and multiple fully observing ring-shaped receivers, where a positive Poiseuille flow exists towards the receivers (Figure 2.1). The Poiseuille flow is a type of parabolic flow that represents the pressure-induced flow of an incompressible viscous fluid in a long narrow duct. The ring-shaped receivers are located on the vessel perimeter and have the same radius (r_v) with vessel and a certain width (w). The receivers can sense their whole projection area or they can sense up to a certain depth. The vessel is considered to be a perfect cylinder with a fully reflecting inner surface.

2.1.1. Diffusion Model

In the diffusion model, the total displacement along the flow direction (ΔX) of a molecule during one simulation time step (Δt) has two dominant factors, namely, displacement due to the diffusion ($\Delta X_{\text{diffusion}}$) and displacement due to the Poiseuille

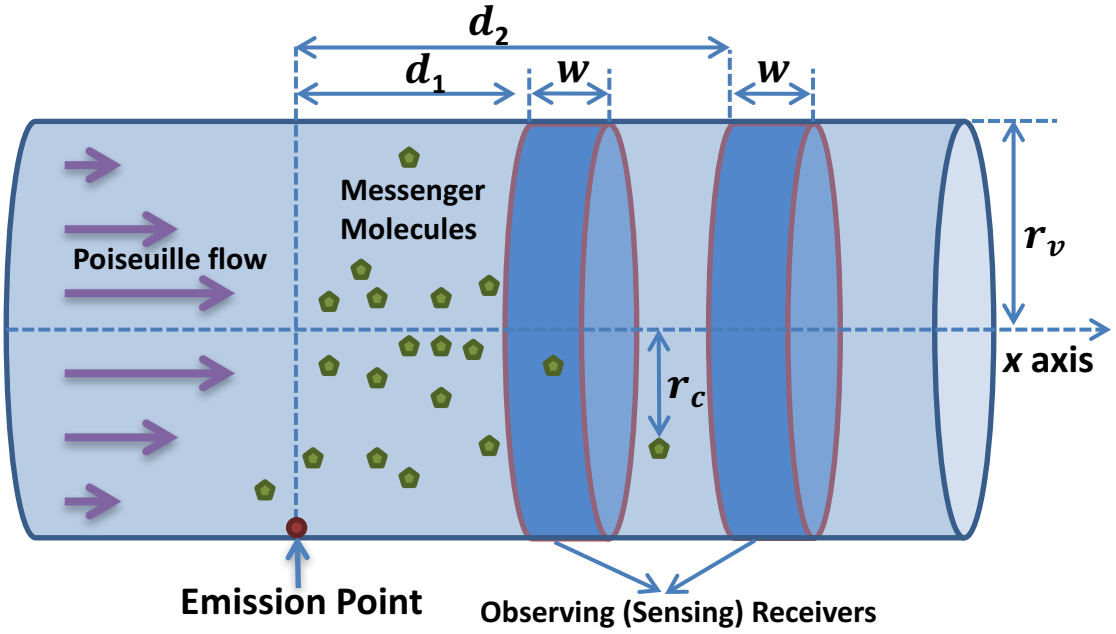

Figure 2.1. Micro-fluidic based communication channel model representation. The derived formulations are independent of the radial location of the emission point.

flow (ΔX_{Pflow}). The displacement due to diffusion follows a Gaussian distribution with

$$\Delta X_{\text{diffusion}} \sim \mathcal{N}(0, 2D\Delta t) \tag{2.1}$$

where D is the diffusion coefficient, and $\mathcal{N}(\mu, \sigma^2)$ is the Gaussian distribution with mean μ and variance σ^2. The displacement due to the Poiseuille flow is calculated as

$$\Delta X_{\text{Pflow}} = v_{pf}(r_c)\,\Delta t \tag{2.2}$$

where $v_{pf}(r_c)$ represents the Poiseuille flow velocity [51] and

$$v_{pf}(r_c) = 2v_m\left(1 - \frac{r_c^2}{r_v^2}\right) \tag{2.3}$$

where v_m is the average flow velocity and r_c is the distance between MM and the central axis of the vessel. Since the flow is not turbulent, it does not have any effect on the other two axes. Therefore, the movement in the y and the z axes are purely diffusion

oriented. Consequently, the total displacement in all three axes in a single time step is

$$\Delta\overrightarrow{r} = (\Delta X_{\text{diffusion}} + \Delta X_{\text{Pflow}}, \Delta Y_{\text{diffusion}}, \Delta Z_{\text{diffusion}}) \tag{2.4}$$

where $\Delta Y_{\text{diffusion}}$ and $\Delta Z_{\text{diffusion}}$ correspond to the displacement in the y and the z axes, respectively, both of which follow a Gaussian distribution as in (2.1).

Another important factor while considering diffusion is the ratio between the advection and the diffusion. This ratio is defined by the Péclet number as

$$\text{Pe} = \frac{\text{advection transport}}{\text{diffusion transport}} = \frac{v_m r_v}{D}. \tag{2.5}$$

As can be seen in (2.5), the movement is more diffusion based for smaller Pe values and vice versa. For instance, Pe = 0 represents pure diffusion. While studying this topology, we consider diffusion dominated movement, so the following constraint is ensured [52]

$$\text{Pe} \ll 4\frac{d_1}{r_v} \tag{2.6}$$

where d_1 is the distance between the transmitter and the closest receiver.

2.1.2. Channel Model

The probability for a molecule to be at a certain d distance from the emission point at time t is written as [52]

$$p(d,t) = \frac{1}{\sqrt{4\pi D_e t}} e^{-\frac{(d-v_m t)^2}{4D_e t}} \tag{2.7}$$

given that

$$v_m = \frac{v_{\max} + v_{\min}}{2} \tag{2.8}$$

where $v_{\max}$ is the maximum flow velocity (i.e., flow velocity in the center of the vessel) and $v_{\min}$ is the minimum flow velocity (i.e., $v_{\min} = 0$), and

$$D_e = D\left(1 + \frac{1}{48}\mathrm{Pe}^2\right) \tag{2.9}$$

where D_e represents the effective diffusion coefficient. Note that the validity of D_e depends on the accuracy of (2.6).

By taking the integral of (2.7) between $d_{R,i}$ and $d_{R,i}+w$, we obtain the probability for a molecule to stand between $d_{R,i}$ and $d_{R,i} + w$ (i.e., to be sensed by Ω_i, where Ω_i represents the ith receiver) at a certain t time as

$$\mathbf{P}_{\mathrm{d}}(\Omega_i, t) = \mathrm{erf}\left(\frac{d_{R,i} + w - tv_m}{2\sqrt{D_e t}}\right) - \mathrm{erf}\left(\frac{d_{R,i} - tv_m}{2\sqrt{D_e t}}\right) \tag{2.10}$$

where $d_{R,i}$ and $d_{R,i} + w$ are the starting and ending location of the Ω_i in the x axis, respectively.

2.2. Localization

In this section, we derive the analytical formulations for the transmitter cell localization for two application scenarios, namely, for known and unknown emission times. Note that the derived formulations are independent of the location of the emission point in the y and the z axes.

2.2.1. Scenario With Known Emission Time

If the receiver knows the emission time of the molecules, it can easily calculate $t_{p,1}$, which is the mean peak time that the receiver observes the maximum number of molecules. Clearly, $t_{p,1}$ can also be derived by taking the derivative of (2.10) with respect to time and equating it to zero as

$$\begin{aligned}(d_1 + v_m t_{p,1}) \exp\left(\frac{-(d_1 - v_m t_{p,1})^2}{4D_e t_{p,1}}\right) \\ -(d_1 + w + v_m t_{p,1}) \exp\left(\frac{-(d_1 + w - v_m t_{p,1})^2}{4D_e t_{p,1}}\right) = 0.\end{aligned} \tag{2.11}$$

Taking the natural logarithm of (2.11) yields

$$\begin{aligned}\frac{(d_1 + w - v_m t_{p,1})^2 - (d_1 - v_m t_{p,1})^2}{4D_e t_{p,1}} &= \log\left(\frac{d_1 + w + v_m t_{p,1}}{d_1 + v_m t_{p,1}}\right) \\ &= \log\left(1 + \frac{w}{d_1 + v_m t_{p,1}}\right).\end{aligned} \tag{2.12}$$

By approximating $\log(1 + a) \simeq a$ for small values of a with the assumption of $w \ll d_1 + v_m t_{p,1}$, we can rewrite (2.12) as

$$2d_1^2 + wd_1 + wv_m t_{p,1} - 2(v_m t_{p,1})^2 - 4D_e t_{p,1} \approx 0 \tag{2.13}$$

which can be solved as

$$d_1 \approx \frac{-w + \sqrt{w^2 - 8(wv_m t_{p,1} - 2(v_m t_{p,1})^2 - 4D_e t_{p,1})}}{4}. \tag{2.14}$$

Note that the negative root of (2.13) is not taken into account, since w cannot be negative.

2.2.2. Scenario With Unknown Emission Time

It is possible that the receiver may not know the emission time and consequently cannot accurately calculate the peak time $t_{p,1}$. In other words, when the receiver tries to calculate $t_{p,1}$, there will be an offset time in the measured $t_{p,1}$. This means that the receiver does not know $t_{p,1}$ as well as d_1, so there are two unknowns in (2.14). In order to solve this problem, we introduce a second receiver with width w, whose distance to the transmitter is d_2 and the mean peak time that second receiver observes the maximum number of molecules is $t_{p,2}$. Note that we assume both receivers have the same width for the sake of simplicity; however, the proposed method also works in the case where the widths of the receivers are not equal. Using these parameters, one can adapt (2.14) for the second receiver as

$$d_2 \approx \frac{-w + \sqrt{w^2 - 8(wv_m t_{p,2} - 2(v_m t_{p,2})^2 - 4D_e t_{p,2})}}{4}. \tag{2.15}$$

Note that both of the receivers do not know $t_{p,1}$, $t_{p,2}$, d_1 and d_2 values. However, they do know

$$\begin{aligned} \triangle t_{2,1} &= (t_{p,2} - t_{p,1}) \\ \triangle d_{2,1} &= (d_2 - d_1) \end{aligned} \tag{2.16}$$

where $\triangle t_{2,1}$ is the mean peak time difference that second and first receivers observe, and $\triangle d_{2,1}$ is the distance difference between the transmitter and the receivers. We can rewrite (2.16) as

$$\begin{aligned} t_{p,2} &= t_{p,1} + \triangle t_{2,1} \\ d_2 &= d_1 + \triangle d_{2,1}. \end{aligned} \tag{2.17}$$

Considering (2.14) and (2.15), $t_{p,1}$ can be solved as

$$t_{p,1} = \frac{2\triangle d_{2,1}\sqrt{H} - Y}{4(\triangle t_{2,1}^2 v_m^4 - \triangle d_{2,1}^2 v_m^2)} \tag{2.18}$$

where

$$H = (-4D_e^2 + 2D_e v_m w)(\triangle t_{2,1}^2 v_m^2 - \triangle d_{2,1}^2) + \triangle t_{2,1}^4 v_m^6 - 2\triangle t_{2,1}^2 \triangle d_{2,1}^2 v_m^4 + \triangle d_{2,1}^4 v_m \tag{2.19}$$

and

$$Y = 4D_e(\triangle t_{2,1}^2 v_m^2 + \triangle d_{2,1}^2) - 2\triangle t_{2,1}^3 v_m^4 + \triangle t_{2,1}^2 v_m^3 w + 2\triangle t_{2,1} \triangle d_{2,1}^2 v_m^2 - \triangle d_{2,1}^2 v_m w. \tag{2.20}$$

Once $t_{p,1}$ is obtained, d_1 can also be obtained by using (2.14).

2.3. Experiments and Results

We have obtained the results using the analytical derivations (2.10), (2.14), (2.18), and a particle-based simulator, which keeps track of the messenger molecules' movement in every simulation time step by evaluating the displacement of each MM at every time step as stated in (2.1), (2.2), (2.3), and (2.4). By utilizing the outputs, we analyze the aforementioned channel and the two localization scenarios under different conditions. Unless specified, number of emitted molecules (n_1) is chosen as 10^7, and simulation estimations are found by taking the average of 1000 simulation replications. The environment parameters are inspired by [1, 13], and Δt is chosen as 0.1 ms.

2.3.1. Channel Model Analysis

First of all, we have tested the validity of the proposed analytical derivation for the channel model in (2.10) by analyzing the change in the percentage of the sensed molecules with time. First, we vary D, v_m, and d_1 values while r_v is equal to 5 µm in Figure 2.2. As expected, for the same v_m values, peak time is observed earlier for higher D values. Also, with the decreasing d_1 values, peak time is again observed earlier. Second, we analyze our proposed channel model by again varying D, v_m, and d_1 values while r_v is equal to 2.5 µm in Figure 2.3. We observe that for the same

D and d_1 values, peak time decreases with the increasing flow velocity as it should be. Moreover, both in Figure 2.2 and Figure 2.3, we see that analytical results match with the simulation results. All in all, we validate the channel model in (2.10) with simulations.

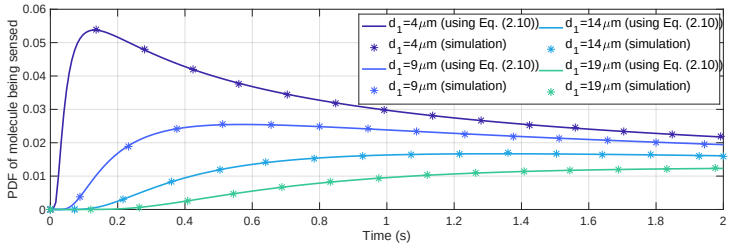

(a) $D = 79.4\,\mu\text{m}^2/\text{s}$, $v_m = 0$

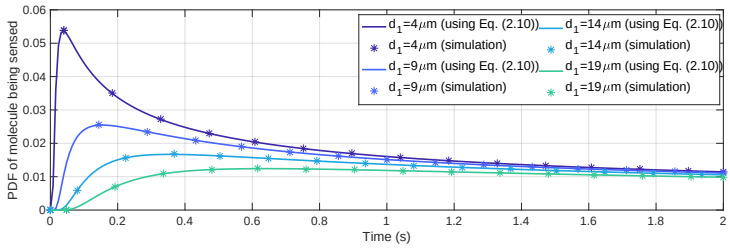

(b) $D = 300\,\mu\text{m}^2/\text{s}$, $v_m = 0$

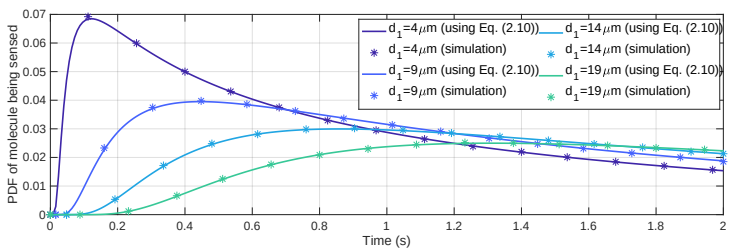

(c) $D = 79.4\,\mu\text{m}^2/\text{s}$, $v_m = 10\,\mu\text{m}\,\text{s}^{-1}$

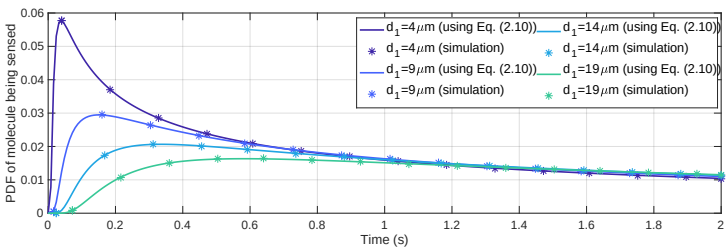

(d) $D = 300\,\mu\text{m}^2/\text{s}$, $v_m = 10\,\mu\text{m}\,\text{s}^{-1}$

Figure 2.2. Time versus probability density function of molecule being sensed while $r_v = 5\,\mu\text{m}$ $(w = 1\,\mu\text{m})$.

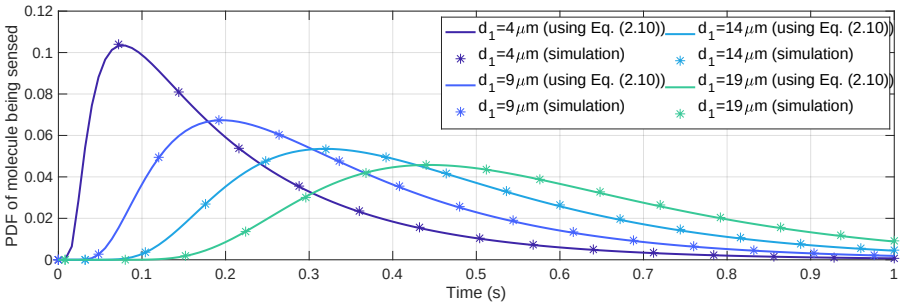

(a) $D = 79.4\,\mu\text{m}^2/\text{s}$, $v_m = 40\,\mu\text{m}\,\text{s}^{-1}$

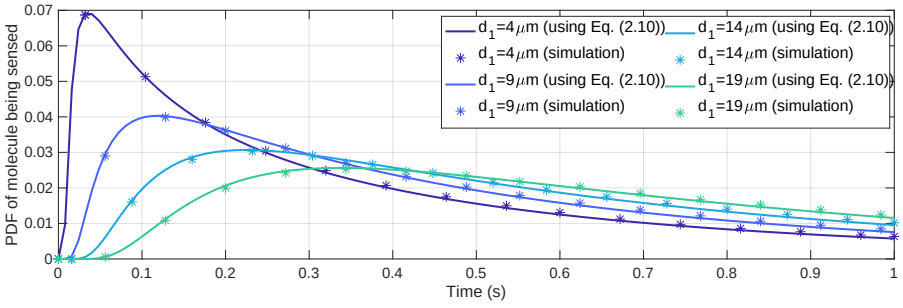

(b) $D = 300\,\mu\text{m}^2/\text{s}$, $v_m = 40\,\mu\text{m}\,\text{s}^{-1}$

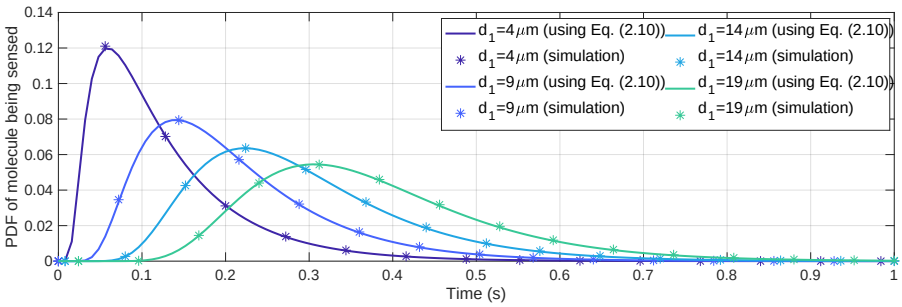

(c) $D = 79.4\,\mu\text{m}^2/\text{s}$, $v_m = 60\,\mu\text{m}\,\text{s}^{-1}$

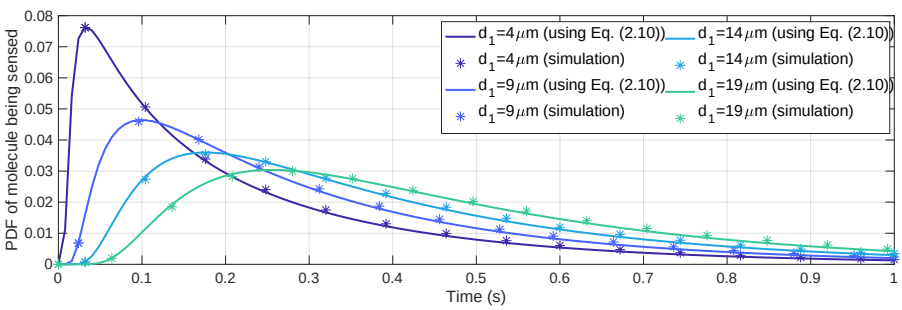

(d) $D = 300\,\mu\text{m}^2/\text{s}$, $v_m = 60\,\mu\text{m}\,\text{s}^{-1}$

Figure 2.3. Time versus probability density function of molecule being sensed while $r_v = 2.5\,\mu\text{m}$ ($w = 1\,\mu\text{m}$).

2.3.2. Localization Analysis for Known Peak-time

Figure 2.4 shows the absolute errors in estimating the distance between the transmitter and the receiver using (2.14). The results show that the absolute error decreases with the increasing d_1 values, which better satisfy (2.6). Furthermore, under the conditions where (2.6) is not strongly satisfied (i.e., for small d_1 values), the distances are estimated with relatively higher absolute errors. Note that the reason for estimating the distance erroneously, even when (2.6) is satisfied, is the $\log(1+a) \simeq a$ approximation. Also from upper lines to lower lines, D_e values increase due to the increase in Pe, which in turn reduces the error. Note that Pe increases with the first power of v_m value, whereas D_e value increases with the second power of v_m value.

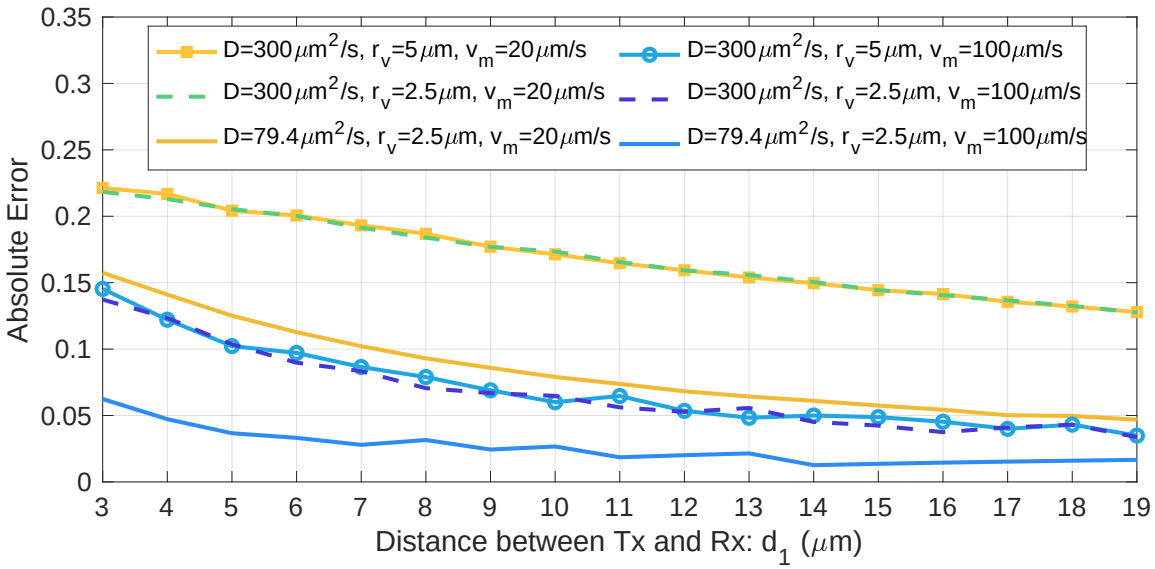

Figure 2.4. Distance versus absolute error for distance estimation considering emission time is known by the receiver (these results are obtained by using the analytical derivation in (2.14)) ($w = 1\,\mu$m).

Figure 2.5 shows the distance estimation results where the transmitter emits few molecules for which the peak times may be observed erroneously. Here, we compare the analytical results with the simulation estimates by varying d_1 and n_1 values, and using the measured peak time $t_{p,1}^{n_1}$ rather than $t_{p,1}$. In the figure, the dashed and the

solid lines represent the distance estimation results via analytical (2.10) and simulation methods. As can be seen in the figure, analytical estimations are pretty close to the actual distances. Distance estimations using simulations diverge slightly for small v_m values because the total amount of sensed data is not large enough to be statistically reliable to measure exact peak time. Moreover, distance estimations using smaller n_1 values diverge even more for larger n_1 values. However, they converge back with the increasing v_m values due to the increasing probability of sensing of the molecules. Also, distance estimations start to diverge after some certain v_m values due to (2.6) no longer being satisfied.

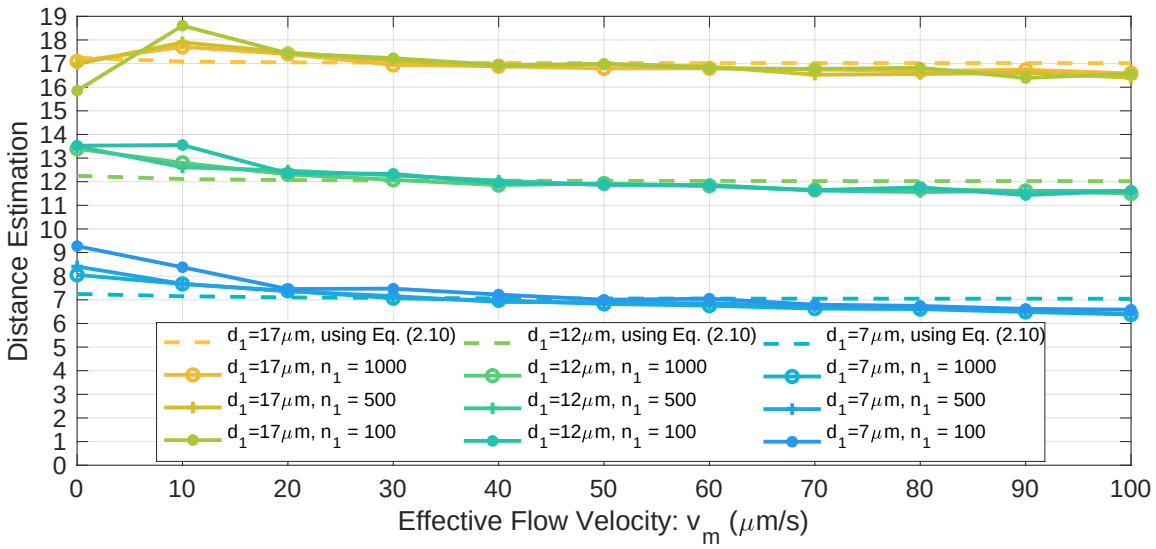

Figure 2.5. Flow versus distance estimation for two cases: (i) using $t_{p,1}$, which is the analytical peak time of the observed molecules (ii) using $t_{p,1}^{n_1}$, which is the peak time obtained by particle-based simulations assuming that n_1 molecules are emitted ($D = 79.4\,\mu\text{m}^2/\text{s}$, $r_v = 5\,\mu\text{m}$, $w = 1\,\mu\text{m}$).

2.3.3. Localization Analysis for Unknown Peak-time

When the emission time is unknown, the peak time can be found using (2.18). After finding the peak time, the distance can be estimated using (2.14). In order to analyze the accuracy of these derived formulations, we select different pairs of receivers

and compare the estimations. As can be seen from Figure 2.6, estimations using the channel model in (2.10) diverge with the increasing v_m values because the condition in (2.6) cannot be ensured for very large v_m values.

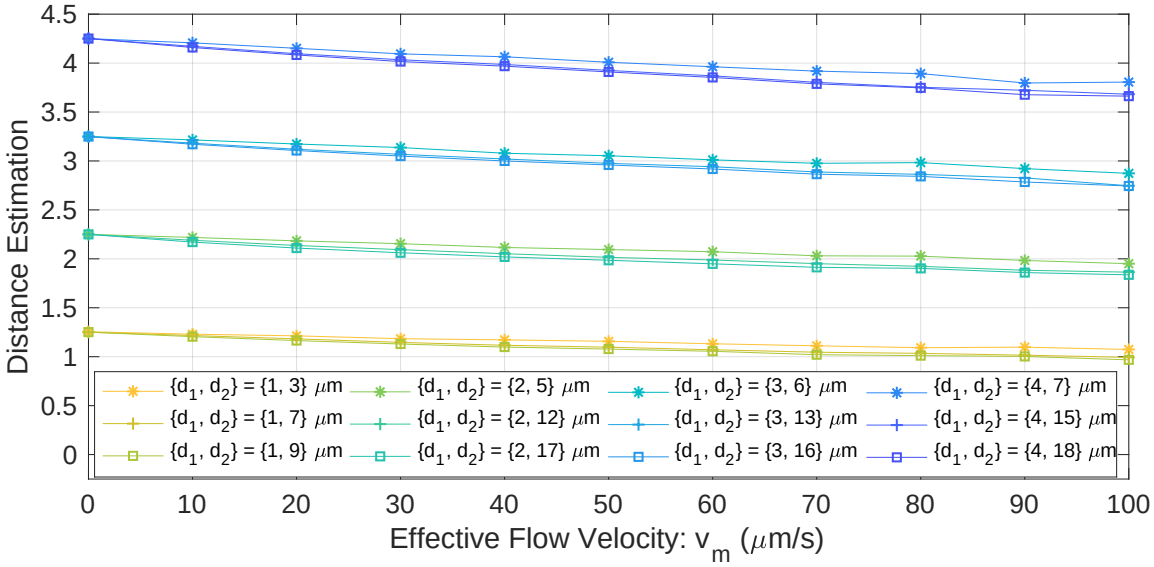

Figure 2.6. Flow versus distance estimation for receivers with different d_1 and d_2 values ($D = 300\,\mu\text{m}^2/\text{s}$, $r_v = 5\,\mu\text{m}$, $w = 1\,\mu\text{m}$).

3. A NEW METRIC FOR THE PERFORMANCE EVALUATION OF A MOLECULAR SIGNAL

As a second main contribution of this thesis, we propose a novel diagram called MOL-Eye to evaluate the performance of a molecular signal. Specifically, we propose three performance metrics based on the MOL-Eye diagram, and named them as maximum eye height (MaxEH), standard deviation of the number of received molecules, and CSNR. We evaluate the validity of these performance metrics by comparing the performance of the classical BCSK modulation technique [14, 15] with an advanced modulation technique that we call BCSK-CPA. BCSK-CPA is based on the BCSK-PA modulation technique, which is proposed in the previous works of the literature [16,17]. According to our simulation results conducted in a 3D vessel-like environment, the three proposed metrics successfully depict the advantage of BCSK-CPA over BCSK, which shows the validity of the proposed metrics in the context of molecular communication via diffusion. Even though we consider a vessel-like environment, the eye diagram and the proposed performance metrics can also be applied to free diffusion environments.

3.1. System Model

Most prior work in the molecular communication literature considers a free diffusion environment where the molecules can roam freely without any boundaries (except the transmitter and the receiver) in the communication environment. In contrast, we consider a cylindrical (i.e., vessel-like) environment with a constant positive flow towards the receiver in this chapter of the thesis. This vessel-like environment is more suitable to model significant *in vivo* and *in vitro* applications such as sensing applications in blood vessels of a human body and micro-fluidic channels. In this chapter, we consider a communication topology consisting of a point transmitter, a fully absorbing circular receiver, a single type of information carrying MM, and a vessel-like environment with uniform flow. The vessel-like environment is considered to be a cylinder with a reflecting surface (Figure 3.1). Since this is a closed environment with a positive flow

towards the receiver, the survival probability of the molecules is much lower than the unbounded environment case. In other words, more molecules are expected to hit the receiver.

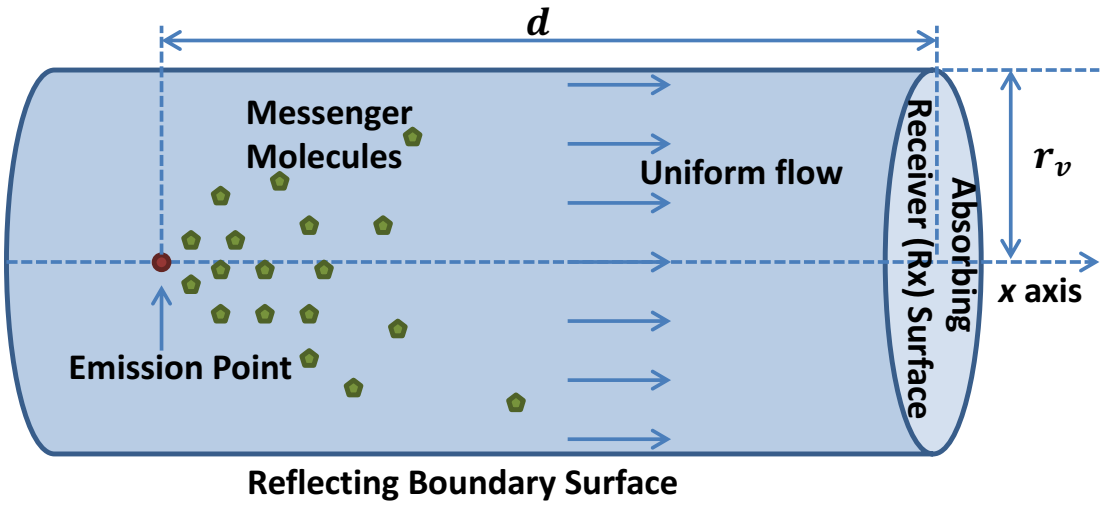

Figure 3.1. Micro-fluidic based communication channel model representation

3.1.1. Diffusion Model

In the diffusion model, the total displacement along the x axis (ΔX) of a messenger molecule in Δt duration is calculated as the sum of the displacement due to the uniform flow (ΔX_{Uflow}) and the displacement due to the diffusion ($\Delta X_{\text{diffusion}}$) as

$$\begin{aligned} \Delta X &= \Delta X_{\text{Uflow}} + \Delta X_{\text{diffusion}} \\ &= v_{uf}\,\Delta t + \Delta X_{\text{diffusion}} \end{aligned} \tag{3.1}$$

where v_{uf} is the uniform flow velocity. As in (2.1), the displacement due to diffusion follows a Gaussian distribution

$$\Delta X_{\text{diffusion}} \sim \mathcal{N}(0, 2D\Delta t) \tag{3.2}$$

where Δt is the simulation time step, D is the diffusion coefficient, and $\mathcal{N}(\mu, \sigma^2)$ is the Gaussian distribution with mean μ and variance σ^2. Considering the movement in

all three axes, the total displacement in a single time step is calculated as

$$\Delta\overrightarrow{r} = (\Delta X_{\text{diffusion}} + \Delta X_{\text{Uflow}}, \Delta Y_{\text{diffusion}}, \Delta Z_{\text{diffusion}}) \tag{3.3}$$

where $\Delta Y_{\text{diffusion}}$ and $\Delta Z_{\text{diffusion}}$ correspond to the displacement in the y and the z axes, respectively, both of which follow a Gaussian distribution with the same μ and σ values with $\Delta X_{\text{diffusion}}$.

3.1.2. Modulation and Demodulation

We use BCSK as the modulation technique with a symbol duration of t_s [15]. In BCSK, a given symbol at the k^{th} symbol duration (i.e., $S[k]$) can either represent bit-0 or bit-1 (i.e., $S[k] \in \{0, 1\}$). Based on this value, the transmitter releases $N^{\text{Tx}}[k]$ molecules where $N^{\text{Tx}}[k] = n_{S[k]}$. In order to increase the detectability of bit-0s and bit-1s, we choose n_0 as 0 and n_1 as the minimum number of molecules sufficient to have a smooth communication.

At the receiver side, $N^{\text{Rx}}[k]$ represents the number of molecules arriving at the receiver within the k^{th} symbol slot, which includes both molecules from the current symbol and the previous symbols. As in (3.4), the receiver applies a basic thresholding on $N^{\text{Rx}}[k]$ to decode the signal ($\hat{S}[k]$) as either bit-0 or bit-1.

$$\hat{S}[k] = \begin{cases} 0, & N^{\text{Rx}}[k] < \lambda \\ 1, & N^{\text{Rx}}[k] \geq \lambda \end{cases} \tag{3.4}$$

In addition to the basic BCSK technique, we have also implemented a variant of BCSK-PA technique proposed in [17] that we call BCSK-CPA. BCSK-PA focuses on minimizing the variation between the $N^{\text{Rx}}[k]$ values where $S[k] = 1$, regardless of the values of the past m symbols (where m is the number of past symbols that are assumed to be affecting the current symbol, which is also called as the ISI window length) by regulating the molecular emission rate. By doing so, BCSK-PA aims to considerably

reduce the effect of ISI in MCvD. To this end, in BCSK-PA, the transmitter uses emission rates based on the past symbol values as

$$\boldsymbol{H}_k^m = (S[k-1], S[k-2], ..., S[k-m]) \tag{3.5}$$

where $\boldsymbol{H}_k^m$ is a vector representing the symbol values of the previous m symbols at the k^{th} symbol slot (i.e., the history of bits at the k^{th} symbol slot) and m is the number of past symbols that are assumed to be affecting the current symbol, which is also called as the ISI window length.

Although BCSK-PA reduces the ISI effect in the communication, it requires a considerable amount of memory at the transmitter side, especially as m increases. For example, if m is equal to 10, 1024 distinct $\boldsymbol{H}_k^m$ cases and corresponding emission amounts are required in BCSK-PA. Our new technique, BCSK-CPA, aims reducing this memory requirement by only considering the cases where the previous symbols have consecutive bit-1s to change the emitted molecule count. Figure 3.2 shows the state diagram of a transmitter utilizing BCSK-CPA with m memory where the state number counts the consecutive bit-1s.

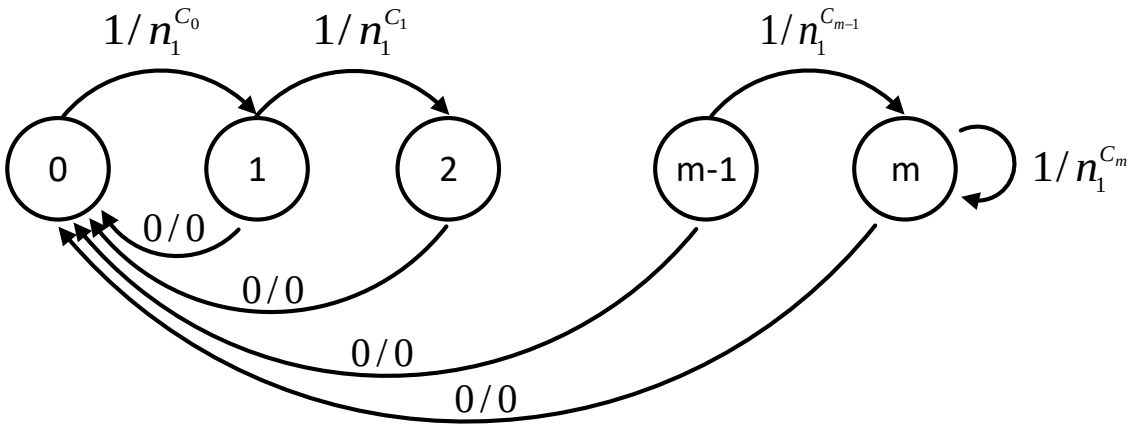

Figure 3.2. State diagram of BCSK-CPA. The state diagram counts the consecutive bit-1s until the current bit. State transitions are given in the form of r/o, where r and o represent $S[k]$ and the $N^{\mathrm{Tx}}[k]$, respectively (e.g., if $S[k] = 1$ when the state is 1, the new state becomes 2 and $n_1^{C_1}$ molecules will be emitted in the current symbol slot).

Furthermore, $\boldsymbol{C}_k$ replaces $\boldsymbol{H}_k^m$ from BCSK-PA and denotes the number of consecutive bit-1s just before the k^{th} symbol slot as

$$\boldsymbol{C}_k = \begin{cases} 0, & S[k-1]=0 \\ 1, & S[k-2]=0\,,\ S[k-1]=1 \\ 2, & S[k-3]=0\,,\ S[k-2]=1\,,\ S[k-1]=1\,. \\ . & . \\ m, & \forall i\ k-m \leq i < k\ S[i]=1 \end{cases} \tag{3.6}$$

The rationale behind BCSK-CPA depends on the fact that in a BCSK system, the effect of bit-0s over ISI is zero. Therefore, we can omit the effect of bit-0s in the past symbol values to reduce the memory requirements of the technique while not considerably impairing the performance of the system.

When molecules are emitted from the emission point, some of them hit the receiver in the current symbol slot while the rest reside in the channel and can be received during the successive symbol slots. We define p_i as the mean fraction of emitted molecules that are received during the i^{th} following symbol slot. Note that p_0 corresponds to the mean fraction of molecules to be absorbed during the current symbol slot. Therefore, the expected number of molecules to be absorbed in the k^{th} symbol slot becomes

$$\mathbf{E}(N^{\mathrm{Rx}}[k]) = p_0 N^{\mathrm{Tx}}[k] + \underbrace{\sum_{i=1}^{m} p_i N^{\mathrm{Tx}}[k-i]}_{\text{residual}} \tag{3.7}$$

where $\mathbf{E}(\cdot)$ is the expectation operator. For BCSK-CPA, the number of molecules to emit is adjusted according to the number of consecutive bit-1s as explained above. Therefore, the expected number of residual molecules ($N_{\mathrm{residual}}[k]$) for the k^{th} symbol

slot becomes

$$\mathbf{E}(N_{\text{residual}}[k]) = \sum_{i=1}^{\boldsymbol{C}_k} p_i N^{\text{Tx}}[k-i]. \tag{3.8}$$

$\mathbf{E}(N_{\text{residual}}[k])$ can be calculated since the transmitted bits are known perfectly by the transmitter. Hence, the number of molecules to emit is adjusted as

$$N^{\text{Tx}}[k] = \begin{cases} n_0 & S[k]=0 \\ n_1^{\boldsymbol{C}_k} = n_1^{\boldsymbol{C}_0} - \frac{\mathbf{E}(N_{\text{residual}}[k])}{p_0} & S[k]=1 \end{cases} \tag{3.9}$$

where $n_1^{\boldsymbol{C}_k}$ denotes the number of molecules to emit when the number of consecutive bit-1s is equal to $\boldsymbol{C}_k$. Note that the calculation in (3.9) ensures having approximately the same number of hitting molecules (at the receiver side) for each bit-1, namely $p_0\, n_1^{\boldsymbol{C}_0}$, which is equal to $p_0\, n_1$.

3.1.3. Formulation of Bit Error Rate

In (3.7), the expected number of received molecules at symbol slot k is given, and $N^{\text{Rx}}[k]$ exhibits a binomial random variable [53]. For tractability, we approximate the binomial random variables with a Gaussian random variable as

$$\begin{aligned} N^{\text{Rx}}[k] &\sim \mathcal{N}(\mu_k, \sigma_k^2) \\ \mu_k &= \sum_{i=0}^{m} p_i\, N^{\text{Tx}}[k-i] \\ \sigma_k^2 &= \sum_{i=0}^{m} p_i\,(1-p_i)\, N^{\text{Tx}}[k-i] \end{aligned} \tag{3.10}$$

where $N^{\text{Tx}}[k-i]$ differs for BCSK-CPA and BCSK. We acquire the p_i values by simulation. Then, we can evaluate the probability of error ($\mathbf{P}_e$) by using Gaussian distribution tail probabilities. Considering the history that includes the previous bits, we obtain

$\mathbf{P}_e$ at the k^{th} symbol slot as

$$\mathbf{P}_e = \mathbf{P}_{e|S[k]=0,\boldsymbol{H}_k^{k-1}}\,\mathbf{P}(S[k]=0,\boldsymbol{H}_k^{k-1}) + \mathbf{P}_{e|S[k]=1,\boldsymbol{H}_k^{k-1}}\,\mathbf{P}(S[k]=1,\boldsymbol{H}_k^{k-1}) \tag{3.11}$$

where $\mathbf{P}_{e|S[k],\boldsymbol{H}_k^{k-1}}$ corresponds to the probability of error given that the history bits are $\boldsymbol{H}_k^{k-1}$ and the current bit is $S[k]$. We evaluate these probabilities with the tail probabilities of the approximate arrival distribution (i.e., the random variable in (3.10)) and considering only the ISI window (i.e., $\boldsymbol{H}_k^m$). Note that we do not need all of the previous bit values to implement BCSK-CPA. However, we need these bit values for the evaluation of BER for analysis purposes.

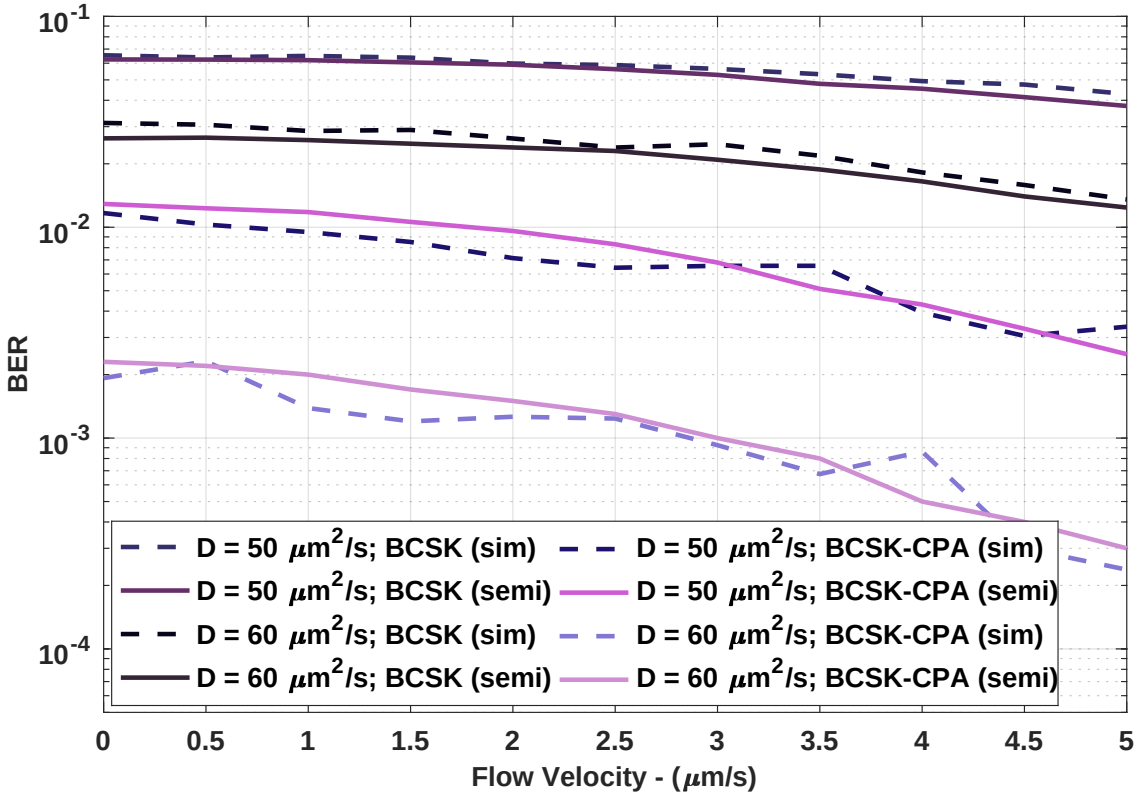

Figure 3.3. BER plot for BCSK and BCSK-CPA. ($d = 6\,\mu\text{m}$, $n_1 = 300$, $t_s = 0.4\,\text{s}$)

In Figure 3.3, we plot the flow velocity versus BER values for the two modulation techniques, namely, BCSK and BCSK-CPA, considering two different diffusion coefficient values. Note that curves with the name *sim* correspond to the simulation results

whereas curves with the name *semi* correspond to the semi-analytical results. In all cases, the simulation and analytical method values are coherent. In other words, simulation results are validated by the analytical method values. Moreover, BCSK-CPA outperforms BCSK by a considerable margin as expected. Additionally, the results show that BER and flow are inversely proportional to one another.

3.1.4. Concept of Eye and MOL-Eye Diagram

Eye diagram, also called as eye pattern, is a method that measures the quality of a signal [54]. It is called as eye diagram because its shape looks like an eye. The width of the eye defines the time interval of the received signal without ISI. Therefore, more open eye implies less ISI level, whereas less open eye implies more ISI level. Eye diagrams are obtained by using oscilloscope, and mostly used by field engineers. Eye diagram is useful for detecting problems such as noise, jitter, and attenuation. The conventional eye diagram has five metrics that are also applicable in MC:

- *0 and 1 level*: The mean values of bit-0 and bit-1 curves in the diagram (dashed lines in Figure 3.4).
- *Rise and fall time*: Transition times of the data to the upward and downward slope of the eye diagram.
- *Eye amplitude*: The biggest distance between the mean of bit-0 and the mean bit-1 curves.

In the context of molecular communication, we propose MOL-Eye as analogous to the eye diagram in conventional communications. As can be seen in Figure 3.4, MOL-Eye is a good way to visualize signals in molecular communication. To obtain the eye diagram in the figure, the received signals of consecutive bit transmissions are repetitively sampled and applied in an overlapping fashion.

In the molecular communication literature, BER is used extensively to measure the quality of the signal. However, BER calculation requires excessive processing power, which would be unsuitable for nanomachines that are expected to have very low energy

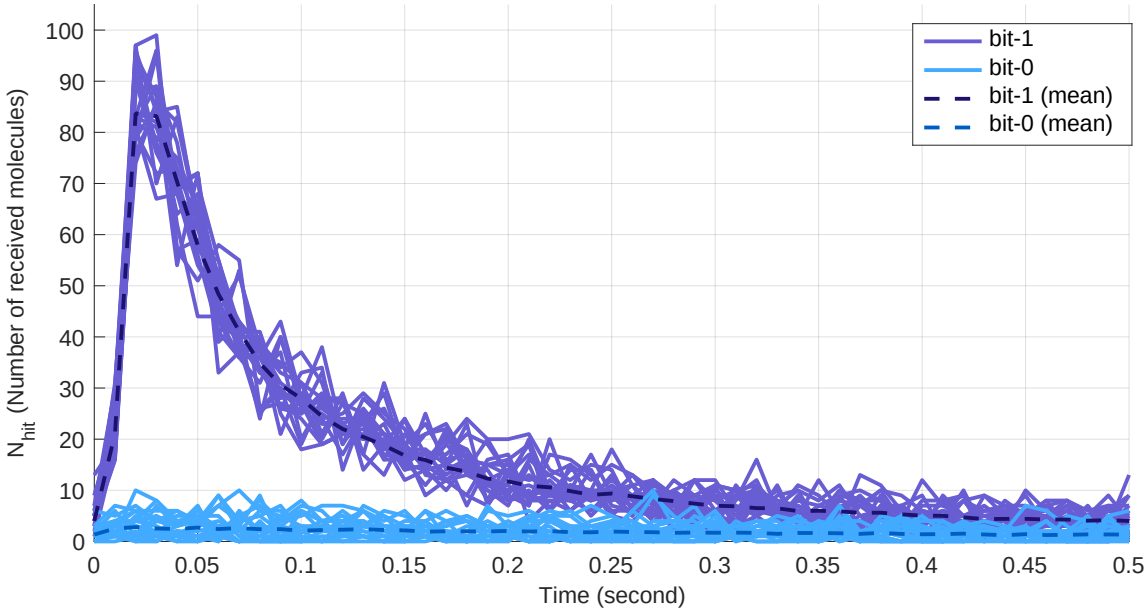

Figure 3.4. A sample eye diagram with BCSK ($r_v = 5\,\mu\text{m}$, $d = 4\,\mu\text{m}$, $t_s = 0.5\,\text{s}$, $D = 150\,\mu\text{m}^2/\text{s}$, $v_{uf} = 5\,\mu\text{m/s}$).

budgets. Therefore, we propose three performance metrics derived from MOL-Eye diagram as alternative performance metrics. We use the conventional eye diagram metric called, maximum eye height (MaxEH), as well as proposing two new metrics for the molecular signal, namely the standard deviation of the received molecules and CSNR. Especially, CSNR is a promising metric since we observe a one-to-one relation between CSNR and BER. Therefore, if the relation between BER and CSNR can be formulated, BER evaluation and optimization process will be much more efficient.

In this thesis, we propose CSNR as a supportive metric to BER. CSNR can be defined shortly as the ratio of the mean and standard deviation of the integral difference between every combination of bit-0 and bit-1 curves. To calculate CSNR, we first define the integral difference between every combination of bit-1 and bit-0 curves as follows

$$\Delta_c(i,j) = \int_0^{t_s} c_1(i) - c_0(j)\,dt \tag{3.12}$$

where $c_1(i)$ and $c_0(j)$ are the ith bit-1 and jth bit-0 sampled curves, and t_s is the symbol duration. Consequently, we calculate the mean (μ_{Δ_c}) and the standard deviation ($STD(\Delta_c)$) of Δ_c values. Finally, we calculate CSNR as in

$$CSNR = \frac{\mu_{\Delta_c}}{STD(\Delta_c)} \tag{3.13}$$

which is an alternative definition of SNR for non-negative signals [55]. As explained above, the messenger molecules are utilized and the number of received molecules are considered as the signal in molecular communication. For this reason, molecular signals are non-negative signals. All in all, our newly proposed alternative SNR definition, CSNR, fits quite well to molecular communication.

3.2. Experiments and Results

The results presented in this section are obtained from the custom-made simulator that keeps track of the hitting molecules, which is the number of successfully received molecules in every simulation time step. By utilizing the simulation output, we evaluate the aforementioned eye diagram metrics and BER values under different conditions.

We consider MCvD in a vessel-like environment as depicted in Figure 3.1. The simulation parameters are given in Table 3.1.

3.2.1. Bit Error Rate Analysis

In Figure 3.5, BER values corresponding to various diffusion coefficient (D) values, number of released molecules for bit-1 transmission (n_1) values, and modulation techniques are presented. According to the figure, BER decreases as D and n_1 values increase. Note that the relative gain of BCSK-CPA compared to BCSK is greater for higher D values.

Since CSNR represents the quality of the signal across noise, it is also expected to be inversely proportional to BER. As can be seen in Figure 3.6, we validate this by

Table 3.1. Simulation Parameters

Parameter	Value
Radius of the vessel (r_v)	5 µm
Radius of the receiver	5 µm
Distance between transmitter and receiver (d)	$\{4, 5, 6\}$µm
Diffusion coefficients (D)	$\{50, 100, 150\}$µm^2/s
Uniform flow velocities (v_{uf})	$0 \sim 5$µm/s
Simulation time step (Δt)	0.1 ms
n_1 (BCSK), $n_1^{C_0}$ (BCSK-CPA)[a]	$50 \sim 300$
Symbol duration (t_s)	$\{0.4, 0.5\}$s
Bit sequence length	100 bits
Number of replications	250

[a] Until the rest of Chapter 3, for the sake of simplicity, we refer to both n_1 and $n_1^{C_0}$ as n_1.

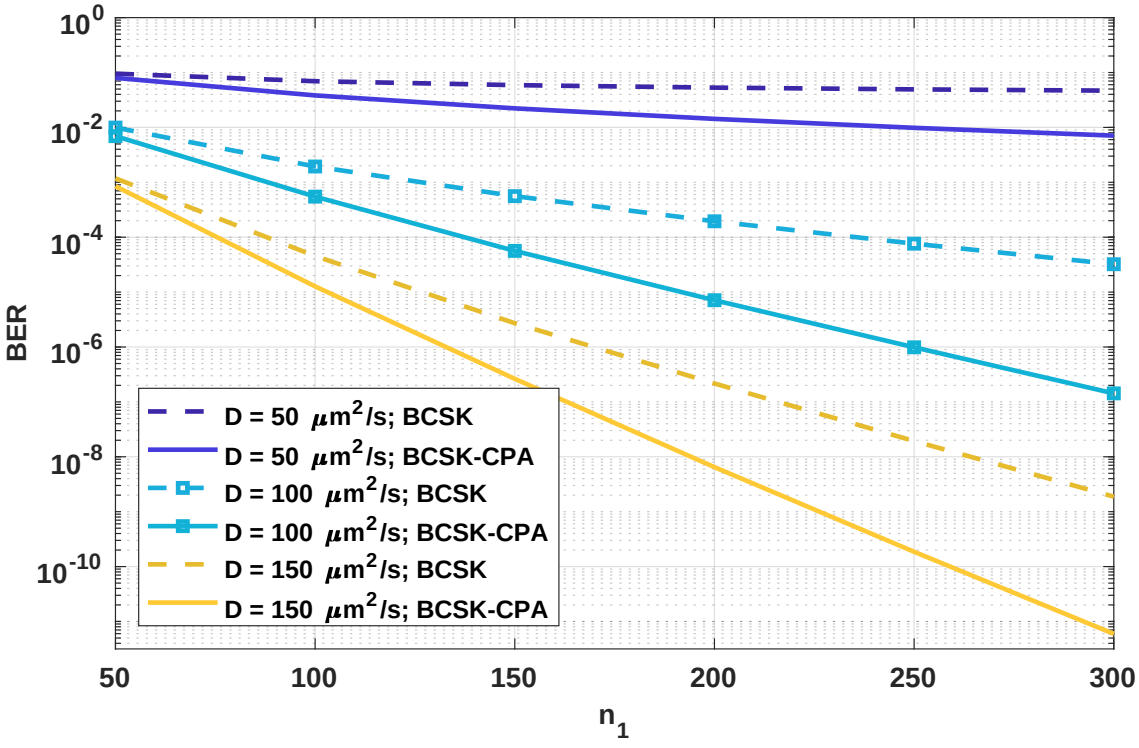

Figure 3.5. Number of molecules vs. BER ($d = 6\,\mu$m, $v_{uf} = 0$, $t_s = 0.4\,$s)

running simulations for 11 different flow values from 0 µm/s to 5 µm/s that are sequentially increased by 0.5 µm/s, three different D values, and two different modulation techniques, namely, BCSK and BCSK-CPA. Finally, we observe that the relation between CSNR and BER is one-to-one for the given parameters, which means BER can be formulated in terms of CSNR. In other words, if the derivations are tractable and can be formulated, BER calculations for concentration shift keying based modulations will be eased.

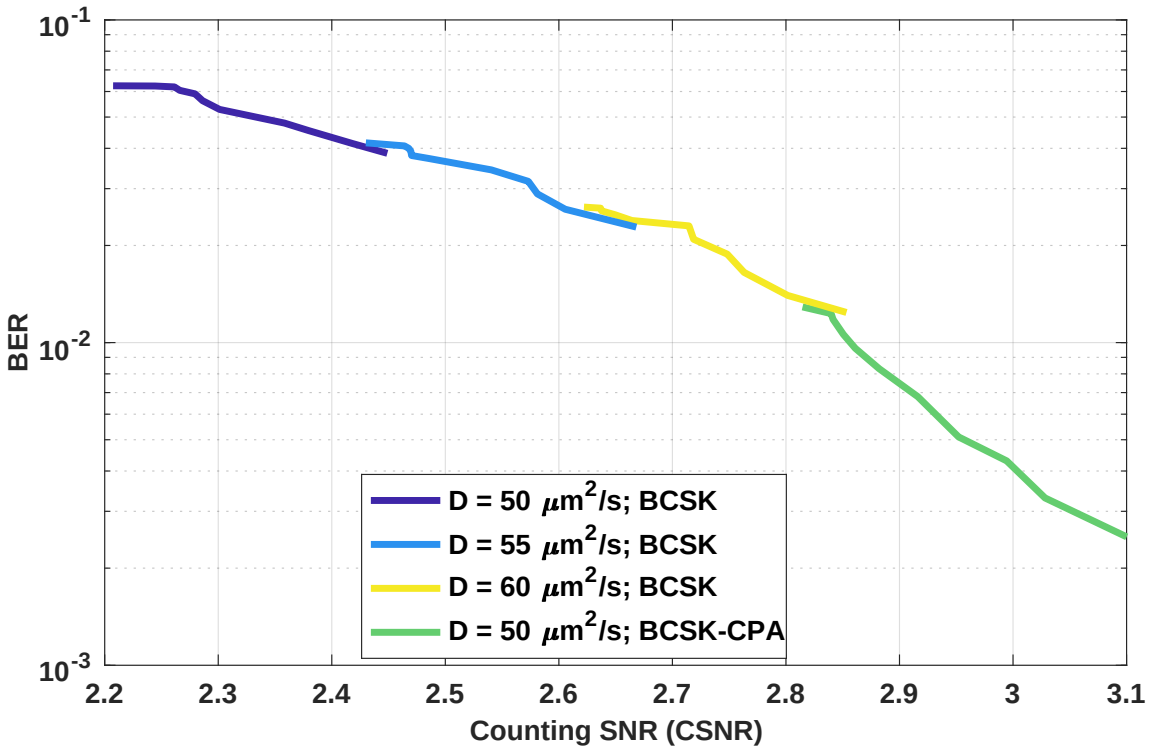

Figure 3.6. CSNR versus BER ($d = 6\,\mu\text{m}$, $v_{uf} = 0 \sim 5\mu\text{m/s}$, $n_1 = 300$, $t_s = 0.4\,\text{s}$)

3.2.2. Eye Diagram Analysis

In the context of MC, we define three new metrics, which are standard deviation of the number of received molecules (STD($c_0(:)$) and STD($c_1(:)$)), maximum eye height (MaxEH), and CSNR. STD($c_0(:)$) and STD($c_1(:)$) are simply calculated by quantifying the amount of variation in the number of received molecules. MaxEH is calculated by finding the maximum distance between the curves of a bit-0 and bit-1 in a single

symbol slot. CSNR is calculated as depicted in (3.12) and (3.13).

In order to test the proposed metrics under different circumstances, we define three different environmental conditions by differing the D, d, and v_{uf} values. D values are inspired by [21], whereas d and v_{uf} values are inspired by the thinnest part of the capillaries [56]. We name defined environments as good, moderate, and harsh, based on the expected quality of communication in the environment. The defined parameters can be seen in Table 3.2.

Table 3.2. Environment Parameters for the Eye Diagram Analysis

Environments	d(µm)	D(µm^2/s)	v_{uf}(µm/s)
Good	4	150	5
Moderate	5	100	2.5
Harsh	6	50	0

Table 3.3 shows the STD($c_0(:)$), STD($c_1(:)$), MaxEH, and CSNR values in these three environments. As can be seen in the table, MaxEH and CSNR increase while the environmental conditions get better or when BCSK-CPA method, which provides smoother communication than BCSK method, is used. In other words, while comparing two different communication environments, we can conclude that the one with the higher MaxEH or CSNR has better communication environment. For the calculation of MaxEH, we normalize the total number of received molecules. For ease of comparison, the metric values of BCSK-CPA in the good environment are given in a bold face font, which represent the best results among six different conditions.

In Figure 3.7, the effect of flow velocities over D values and modulation techniques are depicted. As can be seen in the figure, unlike the relation between BER and flow velocity as in Figure 3.3, CSNR values increase with the rising flow velocities as expected.

Table 3.3. Eye Diagram Metrics

Environments	Metric Name	BCSK	BCSK-CPA
Good	STD($c_0(:)$)	**11.0948**	11.5592
	STD($c_1(:)$)	**29.3192**	29.8338
	MaxEH	**127.6994**	118.0000
	CSNR	**14.5762**	11.6322
Moderate	STD($c_0(:)$)	13.8048	15.1311
	STD($c_1(:)$)	27.2424	29.1996
	MaxEH	68.0454	65.0000
	CSNR	8.5072	6.6060
Harsh	STD($c_0(:)$)	16.0739	19.7512
	STD($c_1(:)$)	22.7202	27.6683
	MaxEH	38.3462	36.0000
	CSNR	3.6683	2.8110

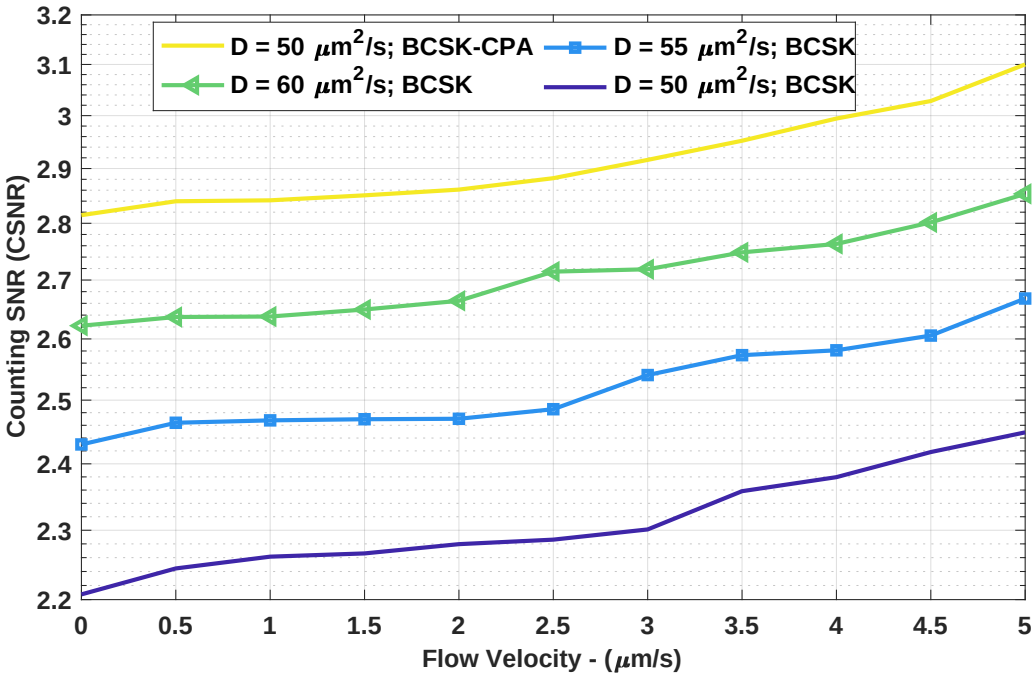

Figure 3.7. Flow velocity versus CSNR ($d = 6\,\mu\text{m}$, $n_1 = 300$, $t_s = 0.4\,\text{s}$)

Finally, the eye diagrams for three different environmental conditions can be seen in Figure 3.8 and Figure 3.9. Curves of bit-1 transmissions are represented in dark blue whereas bit-0 transmissions are represented in light blue. Besides, the diagrams in Figure 3.8 are generated using the BCSK technique, whereas the diagrams in Figure 3.9 are generated using the BCSK-CPA technique. Also, environmental conditions get worse from upper subfigure to lower subfigure, and consequently the openness of the MOL-Eye diagram starts to decrease. The widths are wider in the good environment compared to the moderate and the harsh environments, which shows that the effect of ISI is less in good environment. Moreover, the eyes are also open more in the good environment compared to the moderate and the harsh environments, which shows that there is less noise in the good environment. Please note that the received signals in Figure 3.8 and Figure 3.9 are obtained from consecutive transmissions, and consequently they include ISI.

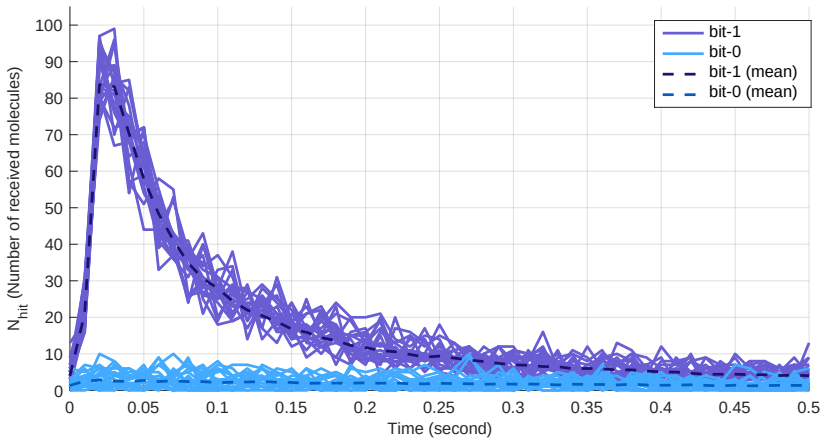

(a) Good environment

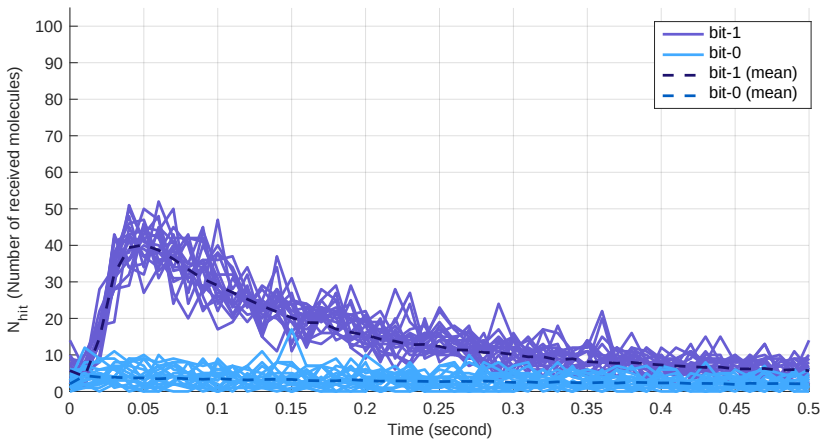

(b) Moderate environment

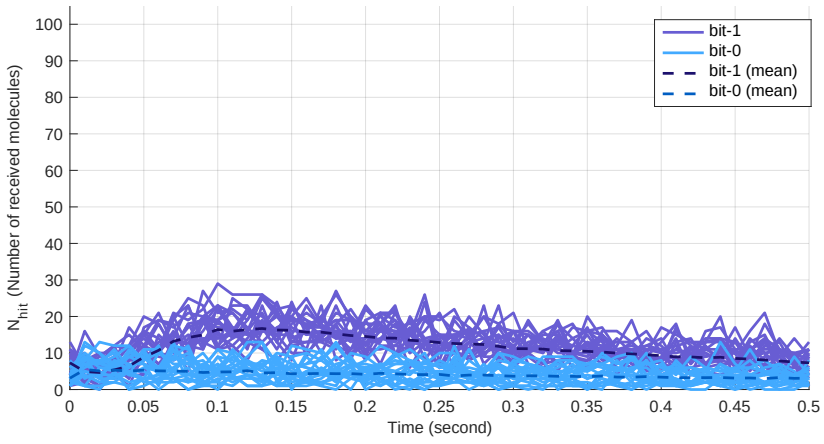

(c) Harsh environment

Figure 3.8. MOL-Eye diagrams of consecutive bit transmissions in different environmental conditions for BCSK ($t_s = 0.5\,\mathrm{s}$).

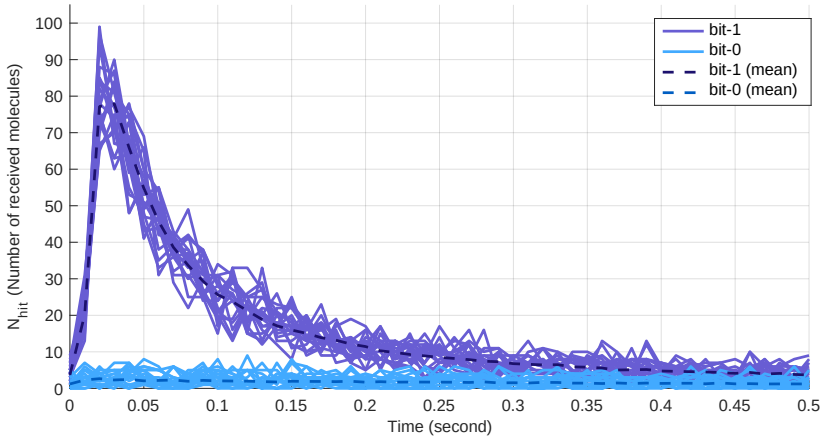

(a) Good environment

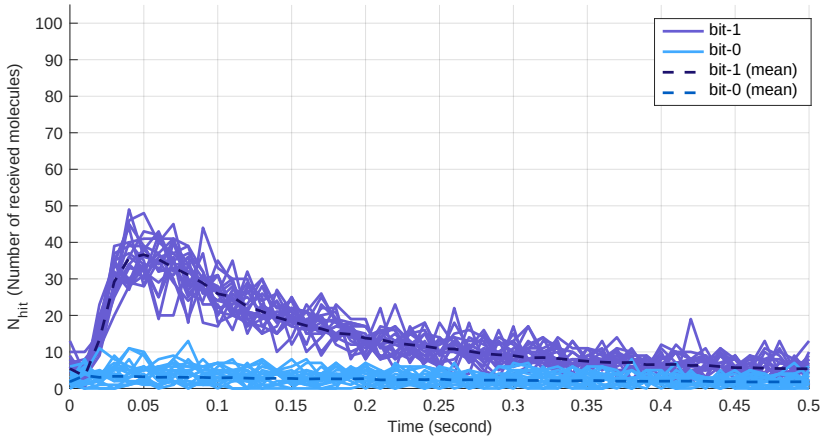

(b) Moderate environment

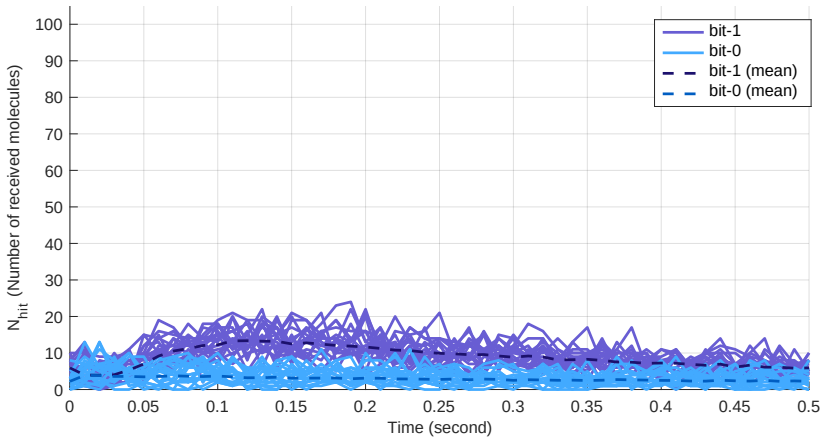

(c) Harsh environment

Figure 3.9. MOL-Eye diagrams of consecutive bit transmissions in different environmental conditions for BCSK-CPA ($t_s = 0.5\,\mathrm{s}$).

4. CHANNEL MODEL OF MOLECULAR COMMUNICATION VIA DIFFUSION IN A VESSEL-LIKE ENVIRONMENT CONSIDERING A PARTIALLY COVERING RECEIVER

As the last main contribution of this thesis, we study the channel model of a vessel-like environment with a partially covering receiver that covers the cross-section of the vessel and vessel walls that reflect the messenger molecules upon collision. In our analysis, we choose a partially covering receiver over a fully covering receiver due to its increased bio-compatibility. While proposing the partially covering receiver, we are inspired by already existing substances in blood vessels such as detecting lipids, bio-markers, and blood clots inside blood vessels. With the aim of channel modeling, the distribution of hitting location of messenger molecules is analyzed. According to the simulation results, we observe that messenger molecules have tendency to be distributed uniformly beyond a certain ratio of the distance to the vessel radius.

4.1. System Model

As in Chapter 2 and Chapter 3, we again consider vessel-like environment in this chapter of the thesis. We consider a diffusion model that consists of a point transmitter, a fully absorbing circular receiver, a single type of information carrying messenger molecule, and a vessel-like environment. The vessel-like environment is considered to be a perfect cylinder with a fully reflecting surface as in Figure 4.1(a).

4.1.1. Diffusion Model

In the diffusion model, since the effect of flow is not considered in this chapter, the only effect that moves messenger molecules is diffusion. Therefore, the total displacement along the x axis (ΔX) of a messenger molecule in a certain Δt duration

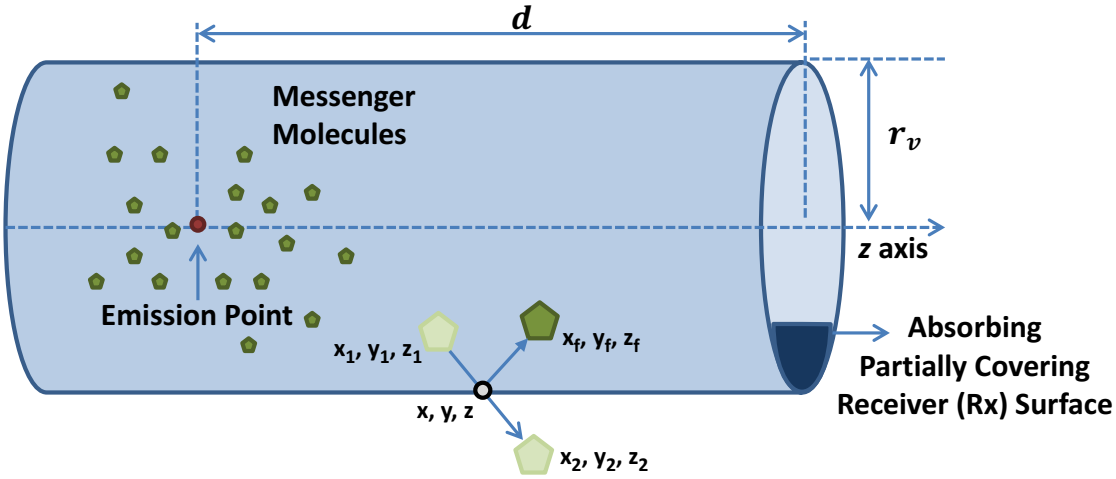

(a) Elastic reflection strategy

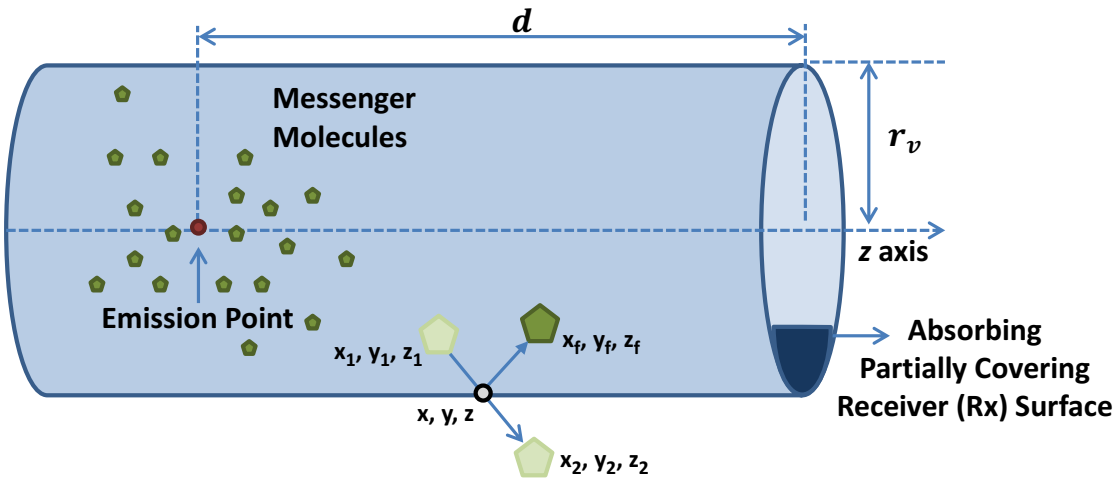

(b) Rollback strategy

Figure 4.1. Micro-fluidic communication channel model and reflection strategies for partially covering and fully reflective boundary surfaces

follows a Gaussian distribution as

$$\Delta X \sim \mathcal{N}(0, 2D\Delta t) \tag{4.1}$$

where Δt is the simulation time step, D is the diffusion coefficient, and $\mathcal{N}(\mu, \sigma^2)$ is the Gaussian random variable with mean μ and variance σ^2. Considering the movement

in all three axes, we can obtain the total displacement in a single time step as

$$\Delta \overrightarrow{r} = (\Delta X, \Delta Y, \Delta Z) \tag{4.2}$$

where ΔY and ΔZ represent the displacement in the y and the z axes, respectively, both of which follow a Gaussian distribution with the same μ and σ^2 values in (4.1).

4.1.2. Reflection Strategies for Fully Reflective Boundary Surfaces

There are two common simulation implementation strategies for the fully reflective vessel surface in the molecular communication literature, namely, rollback and elastic reflection strategies. The most commonly used one is the rollback strategy. In the rollback strategy, as the name suggests, the molecules that hit a surface roll back (Figure 4.1(b)). It is easier to implement and faster run times can be achieved when the reflection strategy is chosen as rollback. However, there is a trade off between complexity and accuracy. It is less realistic to implement a cell or vessel reflection strategy as rollback.

The second strategy is to implement reflection as elastic reflection. Molecules that hit a reflective surface make perfectly elastic collision. Due to its accuracy, we utilize elastic reflection in our simulations. In the rest of this subsection, we describe the mathematical representation of the elastic reflection implementation.

In our communication topology, there are two intersection points between the path of a molecule (represented as a line) and a cylinder. Since net displacement in the z axis does not differ after reflection, we can ignore the movement in this axis. Consequently, the equation of the cylinder can be written as

$$(x - x_3)^2 + (y - y_3)^2 = r_v^2 \tag{4.3}$$

where r_v is the radius of the vessel (i.e., cylinder), (x, y) is the intersection point, and (x_3, y_3) is the center of the cylinder. The line that passes through the intersection

points follows the line equation as

$$\begin{aligned} x &= x_1 + (x_2 - x_1)t \\ y &= y_1 + (y_2 - y_1)t \end{aligned} \tag{4.4}$$

where (x_1, y_1) is the location of the molecules at time $m\Delta t$, (x_2, y_2) is the location of the molecules at time $(m+1)\Delta t$ if vessel had no boundaries, and m is a natural number. When the x and y equations are placed in the cylinder equation, we obtain

$$at^2 + bt + c = 0 \tag{4.5}$$

where a, b, and c are

$$\begin{aligned} a &= (x_2 - x_1)^2 + (y_2 - y_1)^2 \\ b &= 2[(x_2 - x_1)(x_1 - x_3) + (y_2 - y_1)(y_1 - y_3)] \\ c &= {x_3}^2 + {y_3}^2 + {x_1}^2 + {y_1}^2 - (x_3 x_1 + y_3 y_1) - r_v^2 \,. \end{aligned} \tag{4.6}$$

Then, the solution for t can be evaluated by finding the roots of (4.5). After that, the intersection points can be calculated by substituting t in (4.4). Since there are two intersection points, the one closer to the last position of the molecule should be selected as the actual intersection point. After finding the intersection point, the position of the molecule after collision can be found as

$$\begin{aligned} x_f &= 2x - x_2 \\ y_f &= 2y - y_2 \\ z_f &= z_2 \end{aligned} \tag{4.7}$$

where (x_f, y_f, z_f) is the location of the molecule after reflection occurred, and z_2 is the location of the molecule in the z axis at time $(m+1)\Delta t$ if vessel had no boundaries.

All in all, perfectly elastic collision is realized due to its rationality despite the complexity and longer simulation time. Please note that this work considers only single

collisions. In other words, Δt should be small enough and r_v should be large enough to avoid multiple bounces in a single step. Yet, simulations using excessively large Δt cause unreliable results even for the boundless case. Also, putting nanomachines into extra slim vessels (at least 10 times thinner than capillaries in terms of radius [56]) may cause vascular occlusion. Therefore, accuracy of the simulation would experience more troubles in such a case.

4.1.3. Partially Covering Receiver

In the literature, the receiver cells are mostly considered to fully cover the vessel in two dimensions (excluding the dimension that MMs propagate) in vessel-like environments [4, 57]. Therefore, the communication channel reduces to 1D channel. However, we believe that designing the receiver cell as partially covering rather than designing it as fully covering has two important advantages, which are preventing potential health problems and realizing relay nodes in the conventional communication systems.

While building a nanomachine for blood vessels, the risk of vascular occlusion should be considered and minimized in the deployment process independent from the application. Even a small inattentiveness may cause serious health problems. Vascular occlusion is a common and extremely important cause of clinical illness, which is the reason of serious amount of deaths in the world [58]. To this end, partially covering receiver should be used to avoid causing vascular occlusion and consequently serious health problems.

The other reason for considering the partially covering receiver is to use the relay node concept in MCvD domain. Since the maximum amount of distance to propagate through the vessel in diffusive vessel-like channels is limited, relay nodes can be used to amplify the signal. By doing so, diffusive vessel-like channels can be used to communicate with much higher distances, which would not be possible without using relay nodes. It is also biologically more friendly since the receiver cell (also the transmitter cell for the next link) has a partially covering structure.

4.2. Experiments and Results

The results presented in this section are obtained from the particle-based simulator that keeps track of the location of the MMs and stores the MMs that arrive at the destination. By utilizing the simulation output, we evaluate the overall distribution of the location of the received molecules under different environmental conditions with the aim of simplifying the channel model via homogeneity of the molecule hitting locations. We consider a diffusive vessel-like channel as depicted in Figure 4.1(a) with a fully covering receiver. The system parameters are given in Table 4.1.

Table 4.1. Simulation Parameters

Parameter	Value
Radius of vessel (r_v)	$2 \sim 5$µm
Distance between transmitter and receiver (d)	$3.4 \sim 10$µm
Diffusion coefficient (D)	$\{100, 200, 400\}$µm^2/s
Simulation time step (Δt)	0.1 ms
Number of released molecules (N^{Tx})	1.5 million

4.2.1. Distribution Analysis of Hitting Location

When the circular receiver fully covers the vessel in two-dimensions, the hitting point of the received molecule has a certain distance and an angle according to the center of the receiver. In order to show the tendency of the molecules to be distributed uniformly in 3D environment, we analyze the distribution both in terms of the angle and the distance of the molecules with respect to the center of the receiver. There are three dimensions to consider while analyzing the hitting location distribution:

- *Distribution in x and y axes*: Distributions in these two axes are used to find the angular distribution.
- *Distribution in the radius*: After the distribution in the angle is analyzed, the remaining parameter is the distance between the hitting molecules and the center

of the receiver, which we describe as axial distance.

By considering these three distributions in two parts, we plan to consider the overall distribution.

4.2.1.1. Angular Distribution Analysis. Since the receiver is expected to be a circle in the vessel-like environments, angular distribution becomes an important factor while analyzing the distribution of the received molecules. While analyzing uniformity in angle, parameters in Table 4.1 are used. In order to analyze the distribution of the received molecules in angle, we additionally define three different environmental conditions by differing D inspired by [21], d and r_v inspired by the thinnest part of the capillaries [56]. The environments defined as good, moderate, and harsh by different parameter values are presented in Table 4.2.

Table 4.2. Environment Parameters for Distribution Analysis

Environments	$D(\mu m^2/s)$	$d(\mu m)$	$r_v(\mu m)$
Good	400	7	5
Moderate	200	8	4
Harsh	100	9	3

Since the number of received molecules are very high, circular receiver is sliced into 180 parts as in Figure 4.2, and the hitting frequencies of these slices are analyzed. Since the molecules move similarly in each direction, the concentration of the slices are expected to be uniform. In the figure, blue lines represents the density of the total number of hitting molecules in that particular slice whereas red lines represent the mean densities. Note that the numbers outside and within the circle represent the degrees and the density of the slices, respectively.

In that sense, mean, standard deviation, and coefficient of variation of the slices for three different environmental conditions (good, moderate, and harsh) are calculated and given in Table 4.3. As seen, the coefficient of variation values are excessively low,

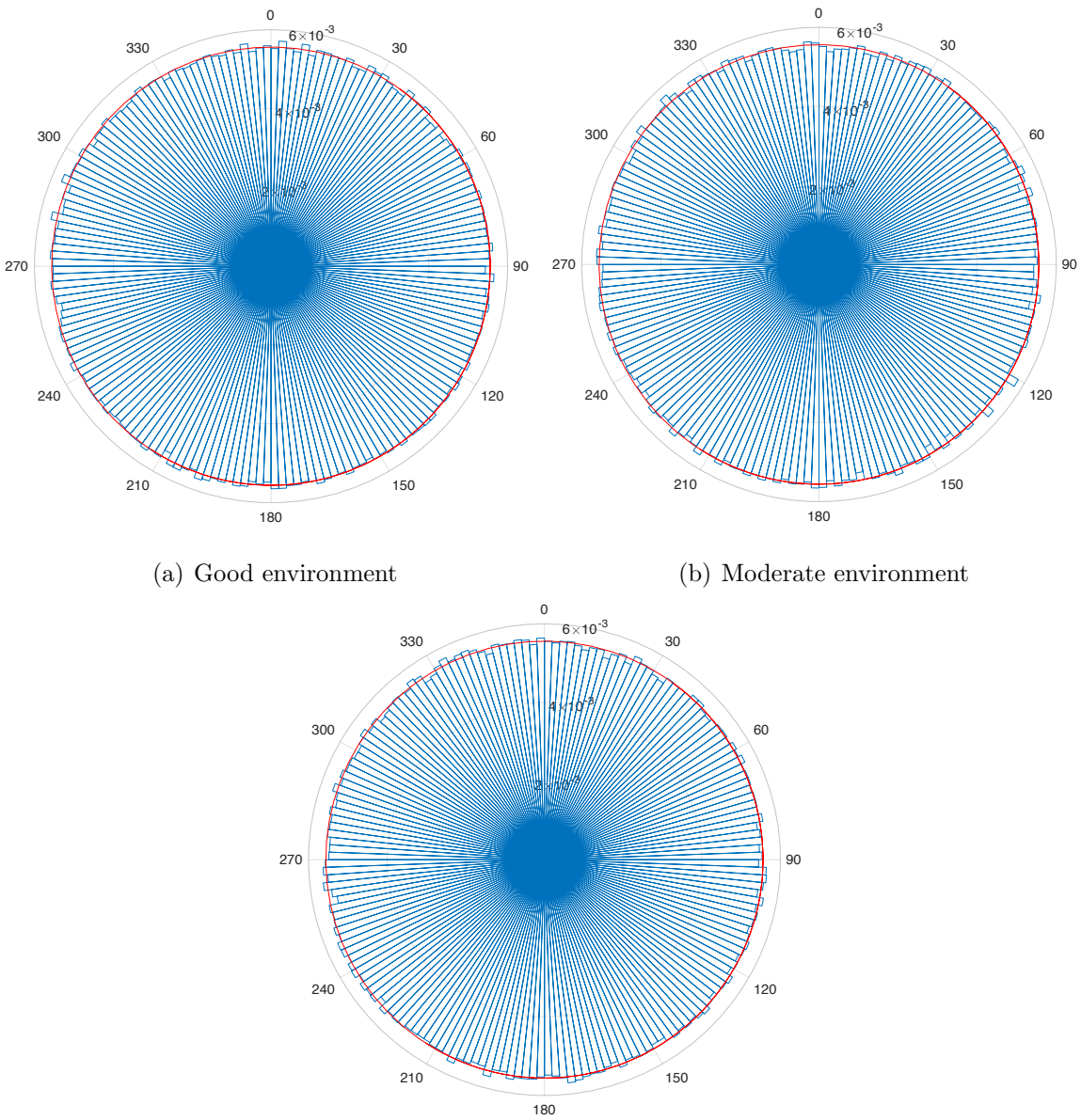

(a) Good environment

(b) Moderate environment

(c) Harsh environment

Figure 4.2. Angular distributions of the received molecules under different environmental conditions.

which means that the deviations from the mean value are negligible. In other words, the MMs have tendency to spread uniformly with respect to the angle. Furthermore, it is shown that the angular distribution is independent from the environmental conditions.

Table 4.3. Metrics of the Angular Distribution Considering 180 Slices

Time	Good Environment	Moderate Environment	Harsh Environment
Mean	5.56×10^{-3}	5.56×10^{-3}	5.56×10^{-3}
Standard deviation	6.44×10^{-5}	7.72×10^{-5}	6.99×10^{-5}
Coefficient of variation	1.16×10^{-2}	1.39×10^{-2}	1.26×10^{-2}

4.2.1.2. Radial Distribution Analysis. Even if the angular distribution is uniform, we also need to consider the uniformity in the axial distance dimension. There may be a case where the slices in angular dimension have a uniform structure but the hitting molecules are mostly close to the center of the receiver. Therefore, considering all the dimensions is crucial for the modeling purposes.

The ratio of the hitting molecules whose axial distances are less than an arbitrary radius r_a to all hitting molecules within a limited time is denoted by $\mathtt{HR}(r_a|t)$, and

$$\mathtt{HR}(\mathtt{r_a}|\mathtt{t}) = \frac{N^{\mathrm{Rx}}(r_a|t)}{N^{\mathrm{Rx}}(r_v|t)} \tag{4.8}$$

where $N^{\mathrm{Rx}}(r|t)$ is the total number of hitting molecules whose axial distances are less than r. Note that for the perfect uniformity, we expect that the molecules hit at each point on the surface with equal probability. In other words, $\mathtt{HR}(\mathtt{r_a}|\mathtt{t})$ should be equal to $(r_a/r_v)^2$ for the perfect uniformity.

In order to ascertain whether the received molecules are spread uniformly or not, one sample Kolmogorov-Smirnov (K-S) test is applied by comparing the perfect uniformity case with the empirical distribution function from simulations. For the significance levels of the K-S test, 5% and 1% are used. Moreover, in order to make a fair comparison between environments with different diffusion coefficients, multiples of

peak times (t_p) are used as the time parameter where $t_p = \frac{d^2}{6D}$ [59].

As the result of the simulations under three different D values, five different r_v values, and 15 different d values, we find that all the test scenarios pass the K-S test when d/r_v is greater than a specific value (Table 4.4). Note that d represents the distance between the transmitter and the receiver, not the whole length of the vessel. Also, d/r_v values in Table 4.4 represent the minimum needed ratio between the transmitter-receiver distance and the radius of the vessel.

Table 4.4. Kolmogorov-Smirnov Test Results

Symbol duration	5% significance level	1% significance level
1-peak time	$d/r_v \geq 2.00$	$d/r_v \geq 2.40$
2-peak time	$d/r_v \geq 1.92$	$d/r_v \geq 2.00$
3-peak time	$d/r_v \geq 1.88$	$d/r_v \geq 1.98$
5-peak time and over	$d/r_v \geq 1.82$	$d/r_v \geq 1.90$

4.2.2. Channel Model of Partially Covering Receiver

Due to both extending the communication range and preventing the health problems, considering and modeling the partially covering receiver is at a great importance. Therefore, we propose an approximation for the channel model of vessel-like diffusive channels by considering the scenarios where the hitting MMs are dispersed homogeneously on the cross-section of the vessel.

As shown in Table 4.4, when we have d/r_v greater than a specific value, the hitting molecules are distributed uniformly. Therefore, in our proposed channel model, we scale 1D formulation by the ratio of the partially covering receiver area to the whole

cross-sectional area as follows

$$F_{\text{hit}}(t) = N^{\text{Tx}}\ \Phi(\Omega)\ \text{erfc}(\frac{d}{\sqrt{4Dt}})$$
$$\Phi(\Omega) = \frac{\text{A}(\Omega)}{\pi r_v^2} \tag{4.9}$$

where $\text{A}(\Omega)$ represents the area of the partially covering receiver Ω. In order to validate (4.9), three different environmental conditions (that passed Kolmogorov-Smirnov test) are considered. As can be seen in Figure 4.3, t_p (which is equal to $\frac{d^2}{6D}$) increases with the increasing d values or decreasing D values, and vice versa. Also, simulation results of both fully and partially receivers perfectly follow the formula stated in (4.9), which is the channel modeling goal of this study.

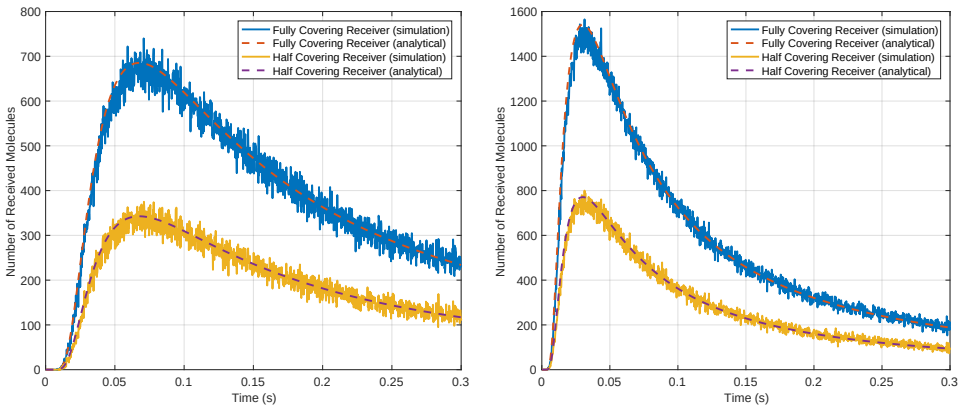

(a) $D = 200$, $r_v = 3$, $d = 9$ (b) $D = 200$, $r_v = 3$, $d = 6$

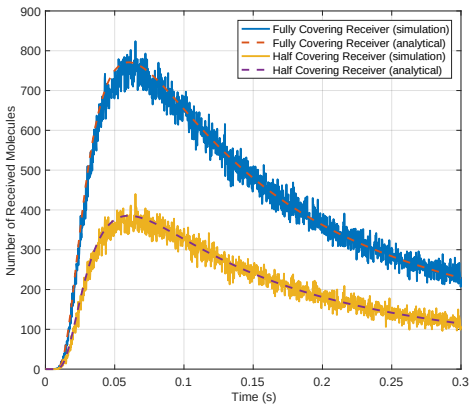

(c) $D = 100$, $r_v = 3$, $d = 6$

Figure 4.3. Time versus number of received molecules for both fully and half covering receivers.

5. CONCLUSION

In this thesis, we have considered vessel-like environment as the communication environment in the context of molecular communication via diffusion. Within that environment, we mainly cover three topics: (1) localization of the transmitter; (2) new metrics and modulation techniques for molecular communication; (3) distribution analysis of hitting location and implementation of a partially covering receiver.

For the localization of the transmitter, we devise the analytical formulations in order to model vessel-like environment and localize the transmitter cell for different application scenarios in diffusion dominated movement. In that sense, we first propose an analytical formulation for the channel model considering a point transmitter, observing receivers that have sensing capabilities through the inside of the vessel, and Poiseuille flow. Using this channel model, we have derived a formulation that calculates the distance between the transmitter and the receiver using a single receiver when the emission time is known. We have also derived an analytical formulation for the unknown emission time case by using two receivers. Finally, we validate the devised analytical framework by using simulations.

For new metrics and modulation techniques for molecular communication, we have proposed a novel metric that we call MOL-Eye diagram based on the conventional eye diagram concept. We introduce three new metrics for performance evaluation using derivatives of MOL-Eye, namely, maximum eye height, standard deviation of the number of received molecules, and CSNR. We show that these metrics can be used to exhibit the quality of different performance enhancement methods in molecular communication. Also, BCSK-CPA modulation technique has been proposed as an alternative power adjustment method to BCSK-PA modulation technique to reduce the memory requirement, which is needed while using BCSK-PA as the modulation technique, by only considering the previous symbols with consecutive bit-1 transmissions. In the experiments, we consider a vessel like environment with uniform flow under three different environmental conditions for two different modulation techniques, namely con-

ventional BCSK and BCSK-CPA. When we compare the performances under different conditions, we confirme that BCSK-CPA outperforms BCSK and the good environment case outperforms the moderate and harsh cases, and so on as expected. Based on our evaluations, we have also seen that CSNR is inversely proportional with BER. Moreover, CSNR and BER have one-to-one relation, which point out that BER can be formulated in terms of CSNR.

As the last contribution of this thesis, we have analyzed hitting location distribution of messenger molecules in a vessel-like diffusive channel. Also, potential application areas and importance of the partially covering receiver are emphasized. Moreover, an approximation for the channel model is given for the cases with uniformly distributed molecule locations, which is assured when the distance between the transmitter and the receiver to the radius of the vessel ratio is very high. Two dimensional distribution of hitting molecules are analyzed in two parts, namely, angular and radial distributions. While analyzing distribution of messenger molecules in radius, radial distribution of messenger molecules are analyzed using Kolmogorov-Smirnov test for two different significance level, namely, 1% and 5%. In order to increase the reliability of the results, more than 100 different environmental conditions are analyzed. All in all, it is shown that molecules that have tendency to spread uniformly in the receiver area beyond certain distance between the transmitter and the receiver to the radius of the vessel ratio. Using these results, we propose a channel model for the partially covering receiver in vessel-like diffusive channels and we verify the channel model by simulations.

REFERENCES

1. Farsad, N., H. B. Yilmaz, A. Eckford, C.-B. Chae and W. Guo, "A Comprehensive Survey of Recent Advancements in Molecular Communication", *IEEE Communications Surveys and Tutorials*, Vol. 18, No. 3, pp. 1887–1919, 2016.

2. Nakano, T., A. W. Eckford and T. Haraguchi, *Molecular Communication*, Cambridge University Press, 1 edn., 2013.

3. Kuran, M. S., H. B. Yilmaz and T. Tugcu, "A tunnel-based approach for signal shaping in molecular communication", *Proceedings on IEEE International Conference on Commununications Workshops (ICC WKSHPS)*, pp. 776–781, 2013.

4. Turan, M., M. S. Kuran, H. B. Yilmaz, C. Chae and T. Tugcu, "MOL-Eye: A New Metric for the Performance Evaluation of a Molecular Signal", *IEEE Wireless Communications and Networking Conference (WCNC)*, pp. 1–6, April 2018.

5. Turan, M., M. S. Kuran, H. B. Yilmaz, I. Demirkol and T. Tugcu, "Channel Model of Molecular Communication via Diffusion in a Vessel-like Environment Considering a Partially Covering Receiver", *IEEE International Black Sea Conference on Communications and Networking (BlackSeaCom)*, pp. 1–5, June 2018.

6. Turan, M., H. B. Yilmaz and T. Tugcu, "Performance analysis of power adjustment methods in molecular communication via diffusion", *IEEE Signal Processing and Communications Applications Conference (SIU)*, pp. 1–4, May 2018.

7. Turan, M., B. C. Akdeniz, M. Şükrü Kuran, H. B. Yilmaz, I. Demirkol, A. E. Pusane and T. Tugcu, "Transmitter Localization in Vessel-like Diffusive Channels using Ring-shaped Molecular Receivers", *IEEE Communications Letters*, Vol. 22, No. 12, pp. 2511–2514, December 2018.

8. Wicke, W., A. Ahmadzadeh, V. Jamali, R. Schober, H. Unterweger and C. Alexiou,

"Molecular communication using magnetic nanoparticles", *IEEE Wireless Communications and Networking Conference (WCNC)*, pp. 1–6, April 2018.

9. Guo, W., T. Asyhari, N. Farsad, H. B. Yilmaz, B. Li, A. Eckford and C.-B. Chae, "Molecular communications: channel model and physical layer techniques", *IEEE Wireless Communications*, Vol. 23, No. 4, pp. 120–127, August 2016.

10. Noel, A., K. C. Cheung and R. Schober, "Diffusive Molecular Communication with Disruptive Flows", *Proceedings IEEE International Conference on Communications (ICC)*, June 2014.

11. Bicen, A. O. and I. F. Akyildiz, "System-Theoretic Analysis and Least-Squares Design of Microfluidic Channels for Flow-Induced Molecular Communication", *IEEE Transactions on Signal Processing*, Vol. 61, No. 20, pp. 5000–5013, July 2013.

12. Klabunde, R. E., *Cardiovascular Physiology Concepts*, Lippincott Williams & Wilkins, 2 edn., 2012.

13. Mohrman, D. E. and L. J. Heller, *Cardiovascular Physiology*, McGraw-Hill Medical, 7 edn., 2010.

14. Kim, N.-R. and C.-B. Chae, "Novel modulation techniques using isomers as messenger molecules for nano communication networks via diffusion", *IEEE Journals on Selected Areas in Communications*, Vol. 31, No. 12, pp. 847–856, December 2013.

15. Kuran, M. S., H. B. Yilmaz, T. Tugcu and I. F. Akyildiz, "Modulation Techniques for Communication via Diffusion in Nanonetworks", *Proceedings IEEE International Conference on Communications (ICC)*, pp. 1–5, June 2011.

16. Einolghozati, A., M. Sardari, A. Beirami and F. Fekri, "Capacity of discrete molecular diffusion channels", *Proceedings IEEE International Symposium on Information Theory (ISIT)*, pp. 723–727, July 2011.

17. Tepekule, B., A. E. Pusane, H. B. Yilmaz and T. Tugcu, "Energy efficient ISI mitigation for communication via diffusion", *Proceedings IEEE International Black Sea Conference on Communications and Networking (BlackSeaCom)*, pp. 33–37, May 2014.

18. Hiyama, S., Y. Moritani, T. Suda, R. Egashira, A. Enomoto, M. Moore and T. Nakano, "Molecular Communication", *Proceedings of NSTI Nanotechnology Conference and Trade Show*, pp. 391–394, 2016.

19. F.Akyildiz, I., F. Brunetti, Cristina and Blázquez, "Nanonetworks: A new communication paradigm", *Elsevier Computer Networks*, Vol. 52, No. 12, pp. 2260–2279, August 2008.

20. Suda, T., M. Moore, T. Nakano, R. Egashira and A. Enomoto, "Exploratory research on molecular communication between nanomachines", *Genetic and Evolutionary Computaion Conference (GECCO)*, pp. 1–5, 2005.

21. Kuran, M. S., H. B. Yilmaz, T. Tugcu and B. Ozerman, "Energy model for communication via diffusion in nanonetworks", *Elsevier Nano Communication Networks*, Vol. 1, No. 2, pp. 86 – 95, 2010.

22. Hiyama, S., R. Gojo, T. Shima, S. Takeuchi and K. Sutoh, "Biomolecular-motor-based nano or microscale particle translocations on DNA microarrays", *ACS Nano Lett.*, Vol. 9, No. 6, pp. 2407–2413, April 2009.

23. Howard, J., A. J. Hudspeth, and R. D. Vale, "Movement of microtubules by single kinesin molecules", *Nature*, Vol. 342, No. 6246, pp. 154–158, November 1989.

24. Dujovne, I., M. V. D. Heuvel, Y. Shen, M. D. Graaff and C. Dekker, "Velocity modulation of microtubules in electric fields", *ACS Nano Lett.*, Vol. 8, No. 12, pp. 4217–4220, October 2008.

25. Kim, E., K. E. Byun, D. S. Choi, D. J. Lee, D. H. Cho, B. Y. Lee, H. Yang, J. Heo,

H. J. Chung, S. Seo and S. Hong, "Electrical control of kinesin-microtubule motility using a transparent functionalized-graphene substrate", *Nanotechnology*, Vol. 24, No. 19, May 2013.

26. Kuran, M. S., T. Tugcu and B. O. Edis, "Calcium signaling: overview and research directions of a molecular communication paradigm", *IEEE Wireless Communications*, Vol. 19, No. 5, pp. 20–27, October 2012.

27. Nakano, T., T. Suda, M. Moore, R. Egashira, A. Enomoto and K. Arima, "Molecular communication for nanomachines using intercellular calcium signaling", *IEEE Conference on Nanotechnology*, pp. 1–4, July 2005.

28. Yilmaz, H. B. and C.-B. Chae, "Simulation study of molecular communication systems with an absorbing receiver: Modulation and ISI mitigation techniques", *Elsevier Simulation Modelling Practice and Theory*, Vol. 49, pp. 136–150, December 2014.

29. Yilmaz, H. B., A. C. Heren, T. Tugcu and C.-B. Chae, "Three-Dimensional Channel Characteristics for Molecular Communications With an Absorbing Receiver", *IEEE Communications Letters*, Vol. 18, No. 6, pp. 929–932, April 2014.

30. Mishra, N., P. Pant, A. Porwal, J. Jaiswal, M. A. Samad and S. Tiwari, "Targeted Drug Delivery: A Review", *American Journal of PharmTech Research*, Vol. 6, No. 1, pp. 1–24, December 2015.

31. Farsad, N., A. W. Eckford, S. Hiyama and Y. Moritani, "On-Chip Molecular Communication: Analysis and Design", *IEEE Transactions on NanoBioscience*, Vol. 11, No. 3, pp. 304–314, September 2012.

32. Azadi, M. and J. Abouei, "A Novel Electrical Model for Advection-Diffusion-Based Molecular Communication in Nanonetworks", *IEEE Transactions on NanoBioscience*, Vol. 15, No. 3, pp. 246–257, March 2016.

33. Wicke, W., T. Schwering, A. Ahmadzadeh, V. Jamali, A. Noel and R. Schober, "Modeling Duct Flow for Molecular Communication", *arxiv preprint arxiv:1711.01479*, 2017.

34. Noel, A., K. C. Cheung and R. Schober, "Optimal Receiver Design for Diffusive Molecular Communication With Flow and Additive Noise", *IEEE Transactions on NanoBioscience*, Vol. 13, No. 3, pp. 350–362, September 2014.

35. Arjmandi, H., M. Zoofaghari and A. Noel, "Diffusive Molecular Communication in a Biological Spherical Environment with Partially Absorbing Boundary", *arxiv preprint arxiv:1810.02657*, 2018.

36. Noel, A., K. C. Cheung and R. Schober, "Improving Receiver Performance of Diffusive Molecular Communication with Enzymes", *IEEE Transactions on NanoBioscience*, Vol. 13, No. 1, pp. 31–43, March 2014.

37. Gerhart, P. M., A. L. Gerhart and J. I. Hochstein, *Fundamentals of Fluid Mechanics*, Wiley, 8 edn., September 2016.

38. Huang, J.-T., H.-Y. Lai, Y.-C. Lee, C.-H. Lee and P.-C. Yeh, "Distance estimation in concentration-based molecular communications", *IEEE Global Communications Conference (GLOBECOM)*, pp. 2587–2591, 2013.

39. Wang, X., M. D. Higgins and M. S. Leeson, "Distance estimation schemes for diffusion based molecular communication systems", *IEEE Communications Letters*, Vol. 19, No. 3, pp. 399–402, 2015.

40. Noel, A., K. C. Cheung and R. Schober, "Joint Channel Parameter Estimation via Diffusive Molecular Communication", *IEEE Transactions on Molecular, Biological and Multi-Scale Communications*, Vol. 1, No. 1, pp. 4–17, August 2015.

41. Lin, L., C. Yang, S. Ma and M. Ma, "Parameter estimation of inverse gaussian channel for diffusion-based molecular communication", *IEEE Wireless Communi-*

cations and Networking Conference (WCNC), pp. 1–6, 2016.

42. Mosayebi, R., A. Ahmadzadeh, W. Wicke, V. Jamali, R. Schober and M. Nasiri-Kenari, "Early Cancer Detection in Blood Vessels Using Mobile Nanosensors", *arxiv preprint arxiv:1805.08777*, 2018.

43. Yilmaz, H. B., N.-R. Kim and C.-B. Chae, "Modulation Techniques for Molecular Communication via Diffusion", *Modeling, Methodologies and Tools for Molecular and Nano-scale Communications*, Vol. 9, pp. 99–118, March 2017.

44. Srinivas, K. V., A. W. Eckford and R. S. Adve, "Molecular Communication in Fluid Media: The Additive Inverse Gaussian Noise Channel", *IEEE Transactions on Information Theory*, Vol. 58, No. 7, p. 4692, April 2012.

45. Singhal, A., R. K. Mallik and B. Lall, "Performance Analysis of Amplitude Modulation Schemes for Diffusion-Based Molecular Communication", *IEEE Transactions on Wireless Communications*, Vol. 14, No. 10, pp. 5681–5691, October 2015.

46. Raut, P. and N. Sarwade, "Connectivity Model for Molecular Communication-Based Nanomachines Network in Normal and Sub-diffusive Regimes", *Proceedings of the International Conference on Computer and Communication Technologies (IC3T)*, pp. 245–256, Springer, September 2015.

47. Jamali, V., A. Ahmadzadeh and R. Schober, "On the Design of Matched Filters for Molecule Counting Receivers", *IEEE Communications Letters*, Vol. 21, No. 8, pp. 1711–1714, August 2017.

48. Mahfuz, M. U., D. Makrakis and H. T. Mouftah, "On the characterization of binary concentration-encoded molecular communication in nanonetworks", *Elsevier Nano Communication Networks*, Vol. 1, No. 4, pp. 289 – 300, 2010.

49. Wang, S., W. Guo and M. D. McDonnell, "Transmit pulse shaping for molecular communications", *IEEE Conference on Computer Communications Workshops*

(INFOCOM WKSHPS), pp. 209–210, April 2014.

50. Chou, C. T., "Molecular circuits for decoding frequency coded signals in nano-communication networks", *Elsevier Nano Communication Networks*, Vol. 3, No. 1, pp. 46 – 56, 2012.

51. Bruus, H., *Theoretical Microfluidics*, Oxford University Press, 1 edn., 2007.

52. Probstein, R. F., *Physicochemical Hydrodynamics: An Introduction*, Wiley-Interscience, 2 edn., 2003.

53. Yilmaz, H. B., C.-B. Chae, B. Tepekule and A. E. Pusane, "Arrival modeling and error analysis for molecular communication via diffusion with drift", *Proceedings ACM International Conference on Nanoscale Computing and Communication (NANOCOM)*, p. 26, 2015.

54. Freude, W., R. Schmogrow, B. Nebendahl, M. Winter, A. Josten, D. Hillerkuss, S. Koenig, J. Meyer, M. Dreschmann, M. Huebner, C. Koos, J. Becker and J. Leuthold, "Quality metrics for optical signals: Eye diagram, Q-factor, OSNR, EVM and BER", *Proceedings International Conference on Transparent Optical Networks (ICTON)*, pp. 1–4, July 2012.

55. Schroeder, D. J., *Astronomical Optics*, Academic Press, 2000.

56. Hall, J. E., *Guyton and Hall Textbook of Medical Physiology*, Elsevier, 13 edn., 2015.

57. Dinc, F., B. C. Akdeniz, A. E. Pusane and T. Tugcu, "A General Analytical Solution to Impulse Response of 3-D Microfluidic Channels in Molecular Communication", *arxiv preprint arxiv:1804.10071*, 2018.

58. Kumar, V., A. Abbas and J. Aster, *Robbins Basic Pathology*, Elsevier, 2017.

59. Schulten, K. and I. Kosztin, *Lectures in Theoretical Biophysics*, Department of

Physics and Beckman Institute, University of Illinois, 2000.